

Synthesis, crystal structures and Hirshfeld analyses of phosphonothioamidates $(\text{EtO})_2\text{P}(=\text{O})\text{C}(=\text{S})\text{N}(\text{H})\text{R}$ ($\text{R} = \text{Cy}, \text{Bz}$) and their coordination on CuI and HgX_2 ($\text{X} = \text{Br}, \text{I}$)

Wafa Arar, Abderrahim Khatyr, Michael Knorr, Lukas Brieger, Anna Krupp, Carsten Strohmann, Mohamed Lotfi Efrif & Azaiez Ben Akacha

To cite this article: Wafa Arar, Abderrahim Khatyr, Michael Knorr, Lukas Brieger, Anna Krupp, Carsten Strohmann, Mohamed Lotfi Efrif & Azaiez Ben Akacha (2021): Synthesis, crystal structures and Hirshfeld analyses of phosphonothioamidates $(\text{EtO})_2\text{P}(=\text{O})\text{C}(=\text{S})\text{N}(\text{H})\text{R}$ ($\text{R} = \text{Cy}, \text{Bz}$) and their coordination on CuI and HgX_2 ($\text{X} = \text{Br}, \text{I}$), Phosphorus, Sulfur, and Silicon and the Related Elements, DOI: [10.1080/10426507.2021.1927032](https://doi.org/10.1080/10426507.2021.1927032)

To link to this article: <https://doi.org/10.1080/10426507.2021.1927032>

 View supplementary material 

 Published online: 21 May 2021.

 Submit your article to this journal 

 Article views: 46

 View related articles 

 View Crossmark data 



Synthesis, crystal structures and Hirshfeld analyses of phosphonothioamidates (EtO)₂P(=O)C(=S)N(H)R (R = Cy, Bz) and their coordination on CuI and HgX₂ (X = Br, I)

Wafa Arar^a , Abderrahim Khatyr^b , Michael Knorr^b , Lukas Brieger^c , Anna Krupp^c , Carsten Strohmann^c , Mohamed Lotfi Efrif^a , and Azaiez Ben Akacha^a

^aSelective Organic and Heterocyclic Synthesis Biological Activity Evaluation Laboratory, Department of Chemistry, Faculty of Sciences, University El Manar, Tunis, Tunisia; ^bInstitut UTINAM-UMR CNRS 6213, Université Bourgogne Franche-Comté, Besançon, France; ^cAnorganische Chemie, Technische Universität Dortmund, Dortmund, Germany

ABSTRACT

The phosphonothioamidates (EtO)₂P(=O)C(=S)N(H)R (**L1** R = Cy; **L2** R = Bz) have been prepared by nucleophilic addition of K[(EtO)₂P(=O)] to R-N=C=S and crystallographically analyzed. Both compounds are associated pairwise through strong intermolecular N-H...O bonding giving rise to 10-membered supramolecular macrocycles. This intermolecular bonding has also been studied by Hirshfeld analysis of **L1** and **L2**. Complexation of **L** on CuI in MeCN solution affords the dinuclear rhomboid-shaped thione complexes [{Cu(μ₂-I)₂Cu}(η¹-L)₂] (**1a,b**). Crystallographic characterization of **1a** reveals that **L1** is ligated exclusively via the thione function to the trigonal Cu(I) centers, which are interconnected through a short Cu-Cu bond of 2.6207(4) Å. In the solid state, individual dimeric complexes are associated through intermolecular N-H...O bonding generating a supramolecular 1D ribbon. The dinuclear complexes [{XHg(μ₂-X)₂HgX}(η¹-L)₂] (**2a** X = Br, L = Cy; **2b** X = Br, L = Bz; **2c** X = I, L = Bz) were formed by stoichiometric addition of **L** to HgX₂. The molecular structures of **2b** and **2c** have been elucidated by X-ray diffraction studies, which show that individual complexes are connected through intermolecular N-H...O bonding generating a supramolecular 1D ribbon. Treatment of **L1** with two equivalents of HgBr₂ produces the tetranuclear compound [Hg₄Br₈(κ¹-L1)₂] **3**, whose unusual bromide-bridged architecture has been elucidated by X-ray crystallography.

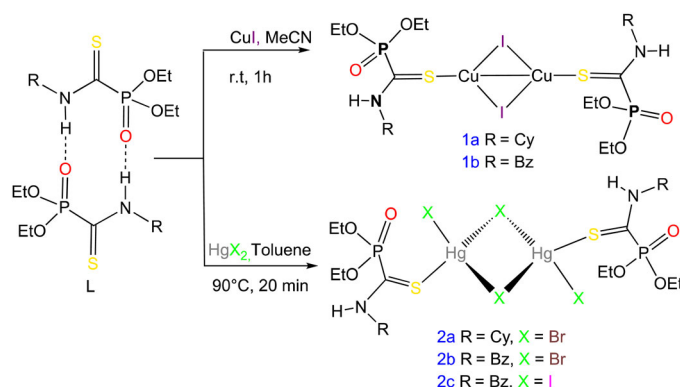
ARTICLE HISTORY

Received 22 February 2021
Accepted 3 May 2021

KEYWORDS

Phosphonothioamidates; crystal structure; Hirshfeld analysis; coordination chemistry; supra-molecular bonding; copper (I); mercury (II)

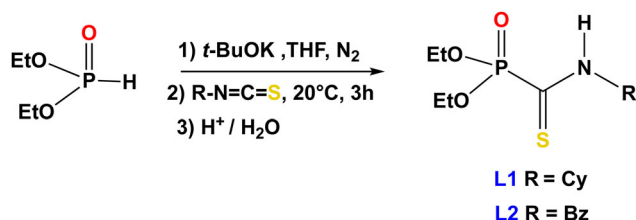
GRAPHICAL ABSTRACT



Introduction

Owing to the important role of α -functionalized phosphonates in different areas such as industry, agriculture, medicine and catalysis, the selective synthesis of these compounds is of interest in organic chemistry.^[1-9] As a subclass, phosphonothioamidates of type (OR)₂P(=O)C(=S)NHR have been recently drawn increasing attention due to their promising biological activity including

herbicidal, antifungal, anticancer, antibiotic, antioxidant and anti-bacterial activity. These compounds are also appearing as pharmaceutically active agents mostly as plant growth regulators, insecticides and selective matrix metalloproteinase inhibitors.^[10-12] Carbamothioylphosphonates have been also reported in organic chemistry as valuable intermediates for the preparation of other synthetic products, such as phosphonothioimidates, *N*-acylphosphonothioamidates, and phosphonoamidines.^[13-18]



Scheme 1. Synthesis of the diethyl *N*-alkylcarbamothioylphosphonates **L1** and **L2**.

Historically, the synthesis of phosphonothioamides (sometimes also named *N*-alkyl or *N*-arylthiocarbamoylphosphonic acid esters or carbamothioylphosphonates) was first reported by Tashma et al.,^[19] which led several groups in the last decades to the development of highly efficient routes for the preparation of these compounds.^[20–24] Among them, the Arbuzov reaction with triethylphosphite and *N,N*-diethyl thiocarbamoyl chloride and the phosphonoformylation of primary amines by triethyl phosphonothioformate have been reported as applicable methods in the literature for the preparation of carbamothioylphosphonates.^[25–31] However, the most widespread approach for the synthesis of phosphonothioamides is the reaction of dialkyl and diaryl phosphites with the appropriate isothiocyanate. Various bases have been used for successful synthesis of these compounds.^[10,27–32] For example, pyridinium perchlorate was found to be an efficient catalyst for the reaction of triethyl phosphite with allylthiocyanate yielding diethyl-*N*-allylthiocarbamoylphosphonate.^[33] Some of us demonstrated recently that potassium *tert*-butoxide may act as efficient base for selective synthesis of phosphonothioamides, which have been used for further transformations such as alkylation with CH_3I affording the corresponding thioimides or *N*-acylation yielding *N*-acyl phosphonothioamide derivatives.^[17,18]

In continuation of that previous work, we report herein the low-temperature structural characterization of diethyl-*N*-cyclohexylthiocarbamoylphosphonate **L1** and diethyl-*N*-benzylthiocarbamoylphosphonate **L2**. A particular attention has been devoted to the ability of these compound to form strong hydrogen bonds.^[34] Since these difunctional compounds feature both hard $\text{P}=\text{O}$ and soft $\text{C}=\text{S}$ donor sites (according to Pearson's HSAB principle)^[35] as potential ditopic ligands for complexation on transition and main group metals, we have focused our investigations on the coordination chemistry of these phosphonothioamides with CuI , HgBr_2 and HgI_2 and present the first examples of dinuclear and tetranuclear metal complexes ligated with **L** and structurally characterized them by four X-ray diffraction studies. The UV-vis and emission spectra of some compounds are also reported.

Results and discussion

The starting materials diethyl-*N*-cyclohexylthiocarbamoylphosphonate **L1** and diethyl-*N*-benzylthiocarbamoylphosphonate **L2** were synthesized by nucleophilic addition of potassium diethyl phosphite (*in situ* generated by deprotonation of diethyl phosphite in the presence of *t*-BuOK) to isothiocyanates using THF as reaction medium. Subsequent

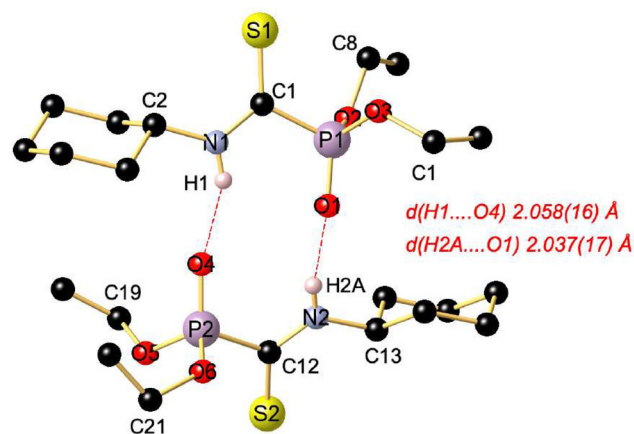


Figure 1. Molecular structure of the hydrogen-bridged dimer of diethyl *N*-cyclohexylcarbamothioylphosphonate (**L1**) in the crystal. Apart from the refined N-H hydrogen atoms, all H atoms are omitted for clarity. Selected bond lengths (Å) and angles ($^\circ$): S1-C1 1.6664(10), P1-O1 1.4725(8), P1-O2 1.5652(8), P1-O3 1.5677(8), P1-C1 1.8242(10), S4-C34 1.6632(10), S2-C12 1.6642(11), N1-C1 1.3305(13), N1-C2 1.4689 (13), C2-C3 1.5247(16), O1-P1-O2 110.09(4), O1-P1-O3 115.79(5), O1-P1-C1 112.00 (5), O2-P1-O3 108.31(4), O2-P1-C1 107.26(5), S1-C1-P1 119.91(6), N1-C1-S1 1127.15(8), N1-C1-P1 112.93(7), N1-C2-C3 109.71(9), C10-O3-P1 121.68(7) and C3-C2-C7 111.30(9).

addition of $\text{H}^+/\text{H}_2\text{O}$ at pH 6 afforded the targeted products in good yield (Scheme 1).^[17]

The NMR spectroscopic data (^1H , ^{31}P , ^{13}C) match with those of related derivatives $(\text{R}'\text{O})_2\text{P}(=\text{O})\text{C}(=\text{S})\text{NHR}$ ($\text{R}'=\text{Me}$, Et), described previously.^[17,18] As exemplified for the hitherto unknown cyclohexyl derivative **L1**, the ^1H NMR spectrum displays along with the sets for the EtO and C_6H_{11} resonances (see Experimental and Figure S1, Supplemental Materials) a broad signal for the NH proton at δ 8.76. Characteristic for the $^{13}\text{C}\{^1\text{H}\}$ NMR spectrum of **L1** is a doublet at δ 192.2 due to the thione carbon atom with a $^1J_{\text{CP}}$ coupling of 179.1 Hz and the observation of a singlet resonance at δ -0.03 ppm (Figures S2 and S3). In the ATR-IR spectrum of **L1** shown in Figure S4, the $\nu(\text{C}=\text{S})$ and $\nu(\text{P}=\text{O})$ vibrations are observed at 1161 and 1230 cm^{-1} . The broadness of the $\nu(\text{N-H})$ adsorption at 3176 cm^{-1} is indicative for strong hydrogen bonding as confirmed by an X-ray diffraction study.

Molecular structure of diethyl *N*-cyclohexylcarbamothioylphosphonate (**L1**)

Yellow single-crystals of **L1** crystallizing in the triclinic space group $\overline{P}1$ were grown from hexane. The unit cell contains 12 molecules, which are pairwise associated to form dimers via strong hydrogen bonding. Figure 1 shows such a dimer formed by hydrogen bonding of two independent molecules through mutual intermolecular $\text{N-H}\cdots\text{O}=\text{P}$ bonding forming a 10-membered supramolecular macrocycle. The $\text{H1}\cdots\text{O4}$ and $\text{H2A}\cdots\text{O1}$ contacts of 2.058(16) and 2.037(17) Å can be considered as strong, and form $\text{N-H}\cdots\text{O}$ angles of 155.9(14) and 166.0(16) $^\circ$, respectively. For the derivative $(\text{MeO})_2\text{P}(=\text{O})\text{C}(=\text{S})\text{N}(\text{H})\text{C}_6\text{H}_4\text{F-}p$, the occurrence of an intramolecular $\text{N-H}\cdots\text{O}$ bonding of only 2.04 Å has been reported. Similar intramolecular interactions are also present in **L1**, but these $\text{N1-H1}\cdots\text{O1}$ and $\text{N2-H2}\cdots\text{O4}$ contacts of

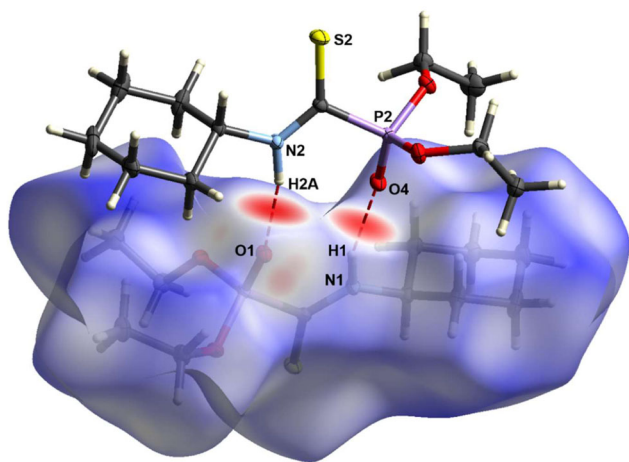


Figure 2. Hirshfeld surface analysis of compound **L1** revealing close contacts in the crystal structure. The strong hydrogen bonds between H1...O4 and H2A...O1 are labeled.

2.423 and 2.600 Å are much weaker than the intermolecular ones. The individual molecules adopt a *s-trans* conformation with respect to the P=O and C=S double bonds, the torsion angles O1–P1–C1–S1 and O4–P2–C12–S2 being 170.35(6) and 154.75(6)°, respectively. A *s-cis* conformation has been reported for the structures of (MeO)₂P(=O)C(=S)N(H)C₆H₄F-*p* and (EtO)₂P(=O)C(=S)N(H)C₆H₅ recorded at ambient temperature; this conformational difference may be due to the different modes of hydrogen bonding (intra- vs. intermolecular). The mean C=S bond length of 1.6653(11) Å is slightly elongated compared to those determined for the latter two derivatives (1.652(3) and 1.648(2) Å).^[17]

For further investigation of the close contacts and intermolecular interactions, a Hirshfeld surface analysis was carried out.^[36] The Hirshfeld surface mapped over d_{norm} in the range from –0.5781 to –1.5733 (arbitrary units) was generated by *CrystalExplorer17*.^[37] As shown in **Figure 2**, the two characteristic red spots indicate the hydrogen bonding of H1...O4 and H2A...O1. One molecule of compound **L1** interacts respectively over two hydrogen bonds to an adjacent one.

Molecular structure of diethyl *N*-benzylcarbamothioylphosphonate (**L2**)

The molecular structure of **L2** has already been described in 1985 by Tashma and Cohen.^[34] Since this structure (CSD refcode DIYWOX) has been recorded at 295 K and was of relatively poor quality, we have redetermined the structure at 100 K and obtained a much better set of crystallographic data. Although the old structure DIYWOX was refined like that of **L2** in the triclinic space group *P*1̄, the angles of the cell parameters of DIYWOX (α 106.75(3), β 108.20(3), γ 81.03(2)) are quite different from those determined for **L2** (α 79.239(3), β 75.131(3), γ 71.391(3)) see Table S1). In contrast to **L1**, the unit cell contains now symmetry-equivalent molecules, which are pairwise associated through intermolecular N–H...O=P bonding forming a 10-membered cycle, as shown in **Figure 3** (top). The H1...O1 distance of 2.099(17)

Å can again be considered as strong, the N–H1...O1 angle of 151.7(16) is somewhat more acute than those of **L1**. The far looser intramolecular N1–H1...O1 contact is equal to 2.428 Å. It is noteworthy to mention that the dimerization encountered in the case of **L1** and **L2** does not apply to all structurally characterized phosphonothioamidate derivatives. For example, compound (EtO)₂P(=O)C(=S)N(H)C₆H₅ **L3** (CSD refcode HABFIC) is associated by a N–H...O=P bridges with two adjacent molecules forming a supramolecular 1D ribbon (**Figure 3**, bottom).^[17] This striking difference between the architectures of **L2** and HABFIC is most probably due to the quite different O=P–C=S torsion angles of the two molecules. The *s-trans* conformation with respect to the P=O and C=S double bonds is now close to ideal *transoid* with a torsion angle O1–P–C8–S of 176.79(6)° for **L2**, whereas in the case of HABFIC the O–P–C–S angle amounts only to 76.5° (*s-cis* conformation).

Also for compound **L2** a Hirshfeld surface analysis was performed with a d_{norm} property over a range of –0.5100 to –1.3188 (arbitrary units). As in the case of **L1**, again two characteristic red spots can be observed (**Figure 4**), indicating the hydrogen bonds H1...O1 between the symmetry-equivalent molecules of **L2**.

Complexation studies

Reactivity of **L1** and **L2** toward copper iodide

Despite the fact that phosphonothioamidates constitute potentially very promising ditopic ligands for coordination chemistry featuring both a hard P=O donor site and a soft C=S donor site, their coordination chemistry has surprisingly never been explored so far. In continuation of our previous work on the reactivity of thione-type organosulfur compounds toward the soft late transition metals Pd(II), Pt(II), Hg(II), Cu(I), Ag(I), and Au(I),^[38–40] we focused for this contribution our investigation on the coordination on CuI and HgX₂ salts. Upon treatment of a solution of CuI in MeCN with **L1** in a 1:1 metal-to-ligand ratio, a fast ligation of **L1** on CuI occurred. After stirring at ambient temperature for 1 h, slow evaporation of the solvent resulted in formation of yellow air stable crystals, which were analyzed by elemental analysis to be a 1:1 adduct (**Scheme 2**). Characteristic for the coordination of the thione function is a slight shift of its C=S band to lower wave number (1156 cm^{–1}). Both the position and broadness of the $\nu(\text{N–H})$ vibration observed at 3151 cm^{–1} indicates that like in **L1** a N–H...O hydrogen bonding occurs (see below). As expected, the ³¹P{¹H} resonance of the (EtO)₂P=O unit at δ –1.4 is not much affected by the ligation ($\Delta\delta$ = 1.4 ppm), since it does not interact with the metal center.

It is well established that CuI forms scarcely mononuclear complexes after ligation with organosulfur ligands (one rare example is [CuI(PCy₃)(2-thioxohexamethyleneimine)],^[41] but rather aggregates to form dinuclear complexes or other higher-nuclear clusters of composition (CuIL)_{*n*} (*n* = 3, 4, 6, 8).^[42–47] A dimerization occurs also during the complexation of **L1** on CuI producing a metal–metal bonded dinuclear species [{Cu(μ_2 -I)₂Cu}(κ^1 -**L1**)₂], as ascertained by an

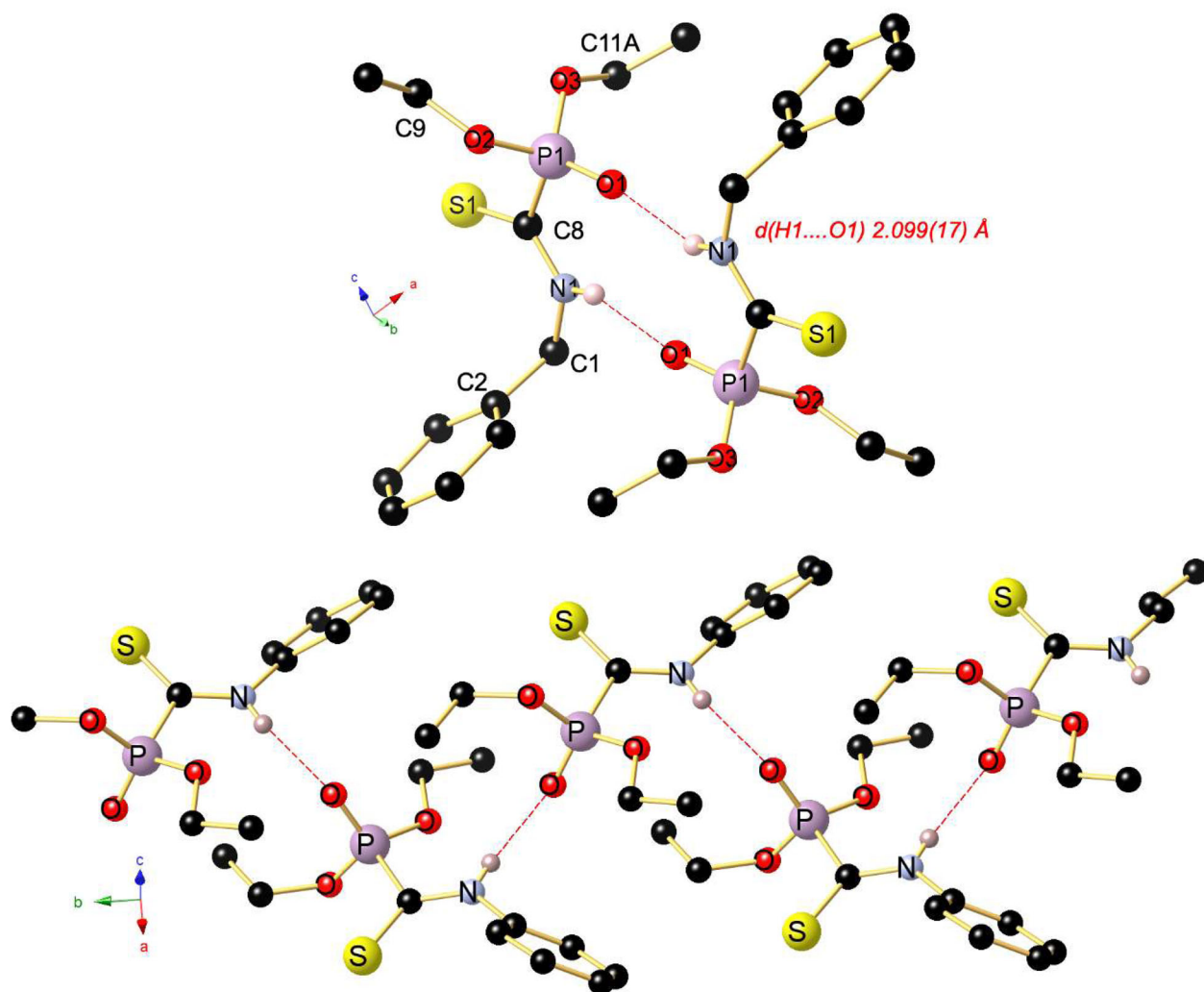


Figure 3. (Top) Molecular structure of the hydrogen-bridged dimer of diethyl *N*-benzylthiocarbamoylphosphonate (**L2**) in the crystal. Apart from the N–H hydrogen atoms, all H atoms are omitted for clarity. Selected bond lengths (Å) and angles (deg): S1–C8 1.6593(10), P1–O1 1.4696(8), P1–O2 1.5666(8), P1–O3 1.5657(8), P1–C8 1.8288(10), O2–C9 1.4598(14), N1–C1 1.4599(13), N1–C8 1.3253(13), C1–C2 1.5124(14), C2–C3 1.3943(14), O1–P1–O2 112.02(5), O1–P1–O3 117.27(5), O1–P1–C8 110.04(5), O2–P1–C8 107.39(5), O3–P1–O2 102.70(4), O3–P1–C8 106.76(5), S1–C8–P1 119.68(6), N1–C1–C2 112.46(8), N1–C8–S1 126.50(8), N1–C8–P1 113.82(7), O2–C9–C10 108.00(10), C3–C2–C1 121.26(10), C7–C2–C1 119.63(9). Symmetry transformation used to generate equivalent atoms: 11-x, 1-y, 1-z. (Bottom) View of a segment of the supramolecular 1D chain of (EtO)₂P(=O)C(=S)N(H)C₆H₅ **L3** in the crystal running along the *b* axis (*d* N–H...O=P 2.089 Å).

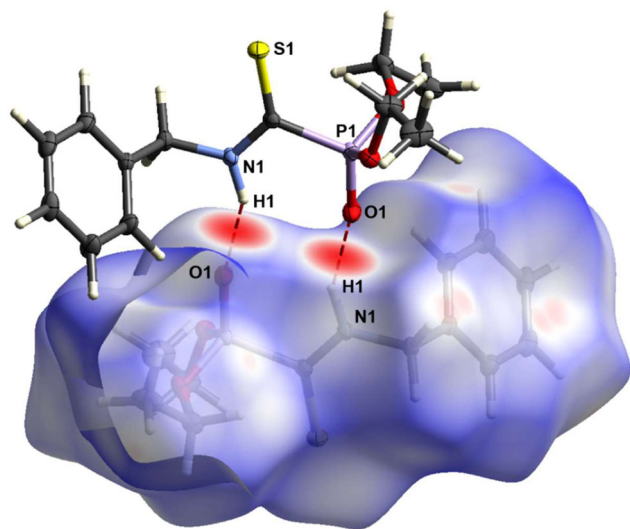
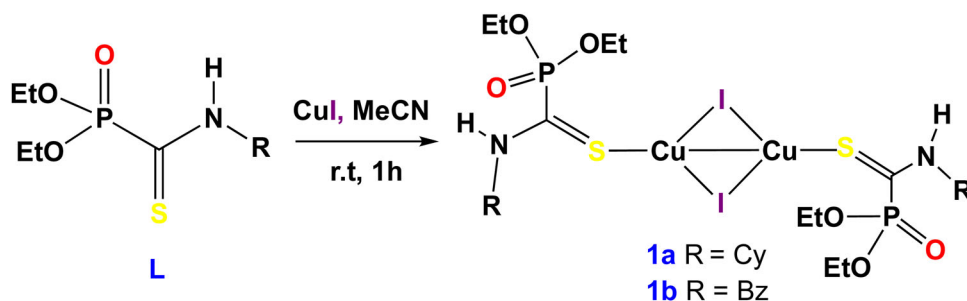


Figure 4. Hirshfeld surface analysis of compound **L2** showing close contacts in the crystal structure. The strong hydrogen bonds between H1...O1 are labeled.

crystallographic characterization (Figure 5). The centrosymmetric molecular structure of **1a** consists of a planar a $\text{Cu}(\mu_2\text{-I})_2\text{Cu}$ rhomboid which is ligated exclusively via the thione function of two *transoid*-arranged **L1** molecules, the torsion angle S–Cu–Cu–S being $174.32(6)^\circ$. There are a couple of other dinuclear copper (I) complexes ligated by thione-type ligands such as the thiosemicarbazone compound $[\text{Cu}_2(\mu\text{-I})_2(\kappa^1\text{-S-Hftsc})_2(\text{PPh}_3)_2]$ (S-Hftsc = $\{(C_4H_3O)(H)C=N-N(H)-C(=S)N(H)Me\}$ (CSD refcode ACIPI), $[\text{Cu}_2(\mu\text{-I})_2(\kappa^1\text{-S-Hptsc})_2(\text{PPh}_3)_2]$ (Hptsc = pyrrole-2-carbaldehydethiosemicarbazone) (CSD refcode AWIRIH), $[\text{Cu}_2(\mu\text{-I})_2(\kappa^1\text{-S-thioacetamide})_4]$ (CSD refcode LAGSIY) or $[\text{Cu}_2(\mu\text{-I})_2(\kappa^1\text{-S-benzenecarbothioamide})_4]$ (CSD refcode TIYZEJ01).^[48–51] However, in all cases, each CuI fragment is tetrahedrally coordinated bearing either a mixed PR_3 -thione donor set or two thione-type ligands. In contrast, in **1a**, each CuI fragment is formally three-coordinate (neglecting the Cu–Cu bond) bearing just a single ligand. We are only aware of only one other dinuclear $\text{SCu}_2\text{I}_2\text{S}$ complex coordinated by a single (and very bulky) monoacylthiourea ligand, namely $\{[\text{Cu}(\mu_2\text{-I})_2\text{Cu}]\{\kappa^1\text{-}$



Scheme 2. Synthesis of the dinuclear complexes **1a** and **1b**.

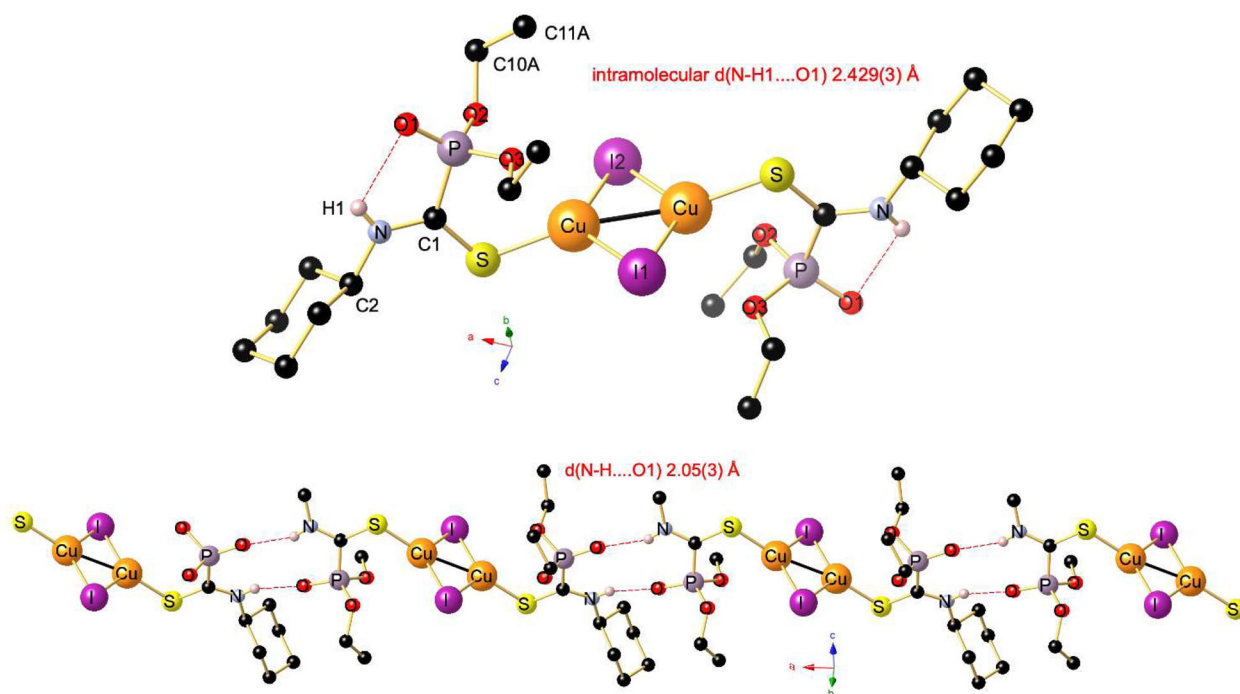


Figure 5. (Top) Molecular structure of **1a** in the crystal. Apart from the N–H hydrogen atoms, all H atoms are omitted for clarity. Selected bond lengths (Å) and angles (°): I1–Cu 2.5781(3), I1–Cu 2.5781(3), I2–Cu 2.5708(3), I2–Cu# 2.5709(3), Cu–Cu# 2.6207(4), Cu–S 2.2561(4), S–C1 1.6791(13), P1–O1 1.4703(11), P1–O2 1.5555(11), N1–C1 1.3154 (16), N1–C2 1.4667(17), C2–C3 1.526(2); Cu–I1–Cu 61.096(9), I1–Cu–Cu 59.452(5), I2–Cu–I1 118.808(8), I2–Cu–Cu 59.356(5), S–Cu–I1 118.914(13), S–Cu–I2 120.344 (13), S–Cu–Cu# 166.228(17), C1–S–Cu 112.04(4), O1–P1–O2 117.44(7), O1–P1–C1 110.46(6), C8–O3–P1 119.60(9), N1–C1–S 124.81(10), S–C1–P1 121.61(7), C1–N1–C2 125.49(11), N1–C2–C3 109.44(11), C3–C2–C7 111.79(11). Symmetry transformation used to generate equivalent atoms: $2-x, +y, 3/2-z$. (Bottom) View of a segment of the supramolecular 1D ribbon of **1a** running along the a axis.

monoacylthiourea)₂] (CSD refcode REQMUY).^[52] There is also [Cu₂I(μ-I)₂Tag₂] coordinated by a morpholinothioamidoguanidine ligand (CSD refcode REJYIQ), but in the latter compound, the pseudo-trigonal Cu(I) centers are additionally stabilized by intermolecular morpholino Cu⋯O contacts.^[53]

A consequence of this low-coordination number may be the extremely short Cu–Cu bond of only 2.6207(4) Å, which may imply a relativistic cuprophilic interaction.^[54,55] Note however that cuprophilicity is still under debates in the literature and advanced computing will be necessary to evaluate the contribution of cuprophilic interactions in the case of complex **1a**.^[55] The Cu–Cu distance within this remarkable complex is even inferior to that of thioether-functionalized tetrathiafulvalene complex [Cu(μ₂-I)₂Cu]{TTF (SMe)₂} (2.6469(15) Å) and [Cu(μ₂-I)₂Cu]{ttht₄} (ttht = tetrahydrothiophene) (2.675(2) Å),^[56,57] and is only 0.06 Å longer than in metallic Cu (2.56 Å). A still shorter intermetallic Cu–Cu bonding of 2.5738(10) has been reported for the above mentioned [Cu(μ₂-I)₂Cu]{κ¹-monoacylthiourea)₂} dimer.^[52] In

contrast, for all tetrahedral dinuclear Cu₂I₂ thione complexes mentioned above, the Cu⋯Cu separation is close or above the sum of the Van der Waals radii of two Cu atoms (2.8 Å).

Although the pseudocyclic array of atoms H1–N–C1–P–O1 is coplanar, there is only a weak intramolecular contact of 2.05(3) Å between the P=O atom and the H–N group (Figure 5, top). But in agreement with the IR spectroscopic data (see above), individual molecules of **1a** are mutually associated *via* strong intermolecular N–H⋯O=P bonding generating an infinite supramolecular 1D ribbon. As shown in Figure 5 (bottom), the hydrogen bonding occurs through pairwise bridging of the N–H⋯O1 atoms forming 10-membered macrocycles. The H1⋯O1 contact of 2.05(3) Å is of similar length as that of **L1**, and forms an N–H⋯O angle of 155.0(3)°. For complex **1a**, also a Hirshfeld surface analysis was performed for the investigation of close contacts and intermolecular interactions. The Hirshfeld surface was mapped over d_{norm} in the range from –1.0410 to –1.3556 (arbitrary units) and is illustrated in

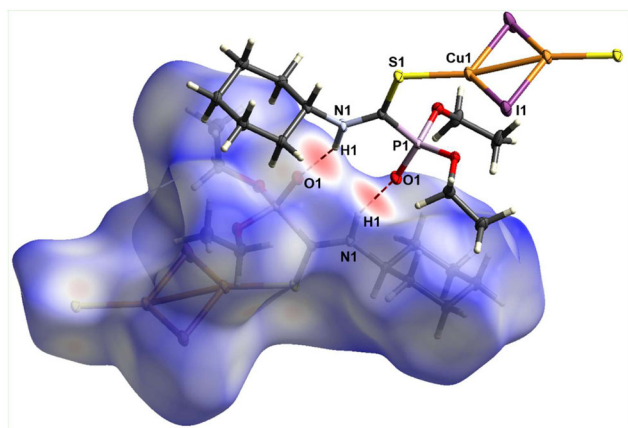


Figure 6. Hirshfeld surface analysis of compound **1a** showing close contacts in the crystal structure. The strong hydrogen bonds between H1...O1 are labeled.

Figure 6. Two characteristic red spots indicate the hydrogen bond H1...O1 between an adjacent molecule of **L1** ligated to Cu₂I₂ core, to build an infinite supramolecular 1D ribbon.

A yellowish crystalline material of composition [Cu(L2)]₂ was also obtained upon treatment of a MeCN solution of CuI with an equimolar amount of **L2** according to Scheme 2. The similarity of the spectroscopic data with those of **1a** makes it reasonable to suggest also a dinuclear structure for [{Cu(μ₂-I)₂Cu}(κ¹-**L2**)₂] **1b**. The occurrence of an intense ν(N-H) vibration at 3210 cm⁻¹ in ATR-IR spectrum indicates that as in **1a** the individual complexes are aggregated via intermolecular N-H...O bridges (Figure S15).

Reactivity of **L1** and **L2** toward mercury (II) halides (X = Br, I)

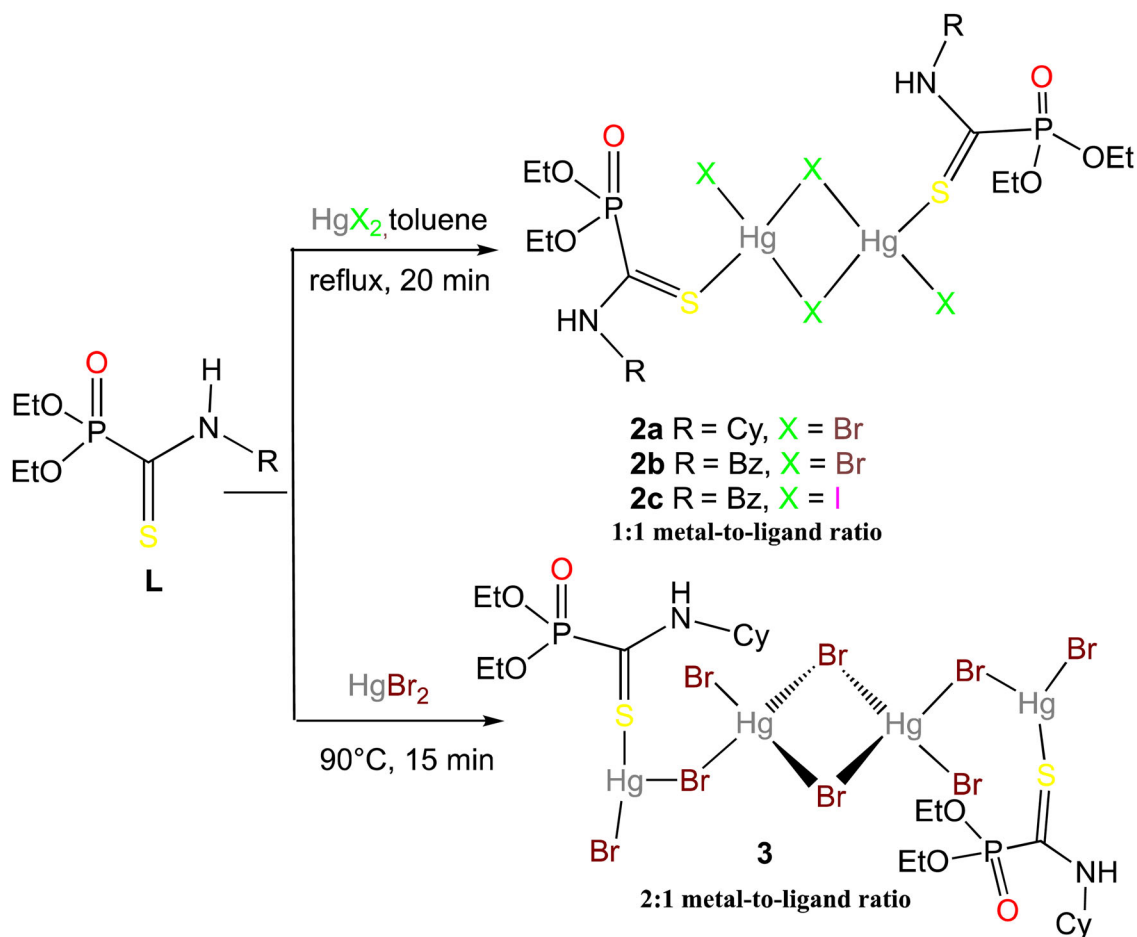
Based on our previous experience on the coordination of thione-type ligands such as 4,5-bis(methylthio)-1,3-dithiole-2-thiones or 1,3-dithiolo-(4,5-*d*)-1,3-dithiol-2,5-dithione on mercury(II),^[38,40,58] we extended our complexation studies of **L** on the soft salts HgBr₂ and HgI₂. Upon heating HgBr₂ with a slight excess of **L1** in refluxing toluene, formation of pale yellowish crystals occurred after allowing the solution to reach ambient temperature. This stable product has according to elemental analysis a [HgBr₂L1] composition (Scheme 3). In the ³¹P{¹H} NMR spectrum, the singlet resonance of metal-ligated **L1** appears now low-field shifted at δ 1.21 with Δδ of 1.24 ppm with respect to free **L1**. The N-H resonance δ 9.47 is also markedly low-field shifted with respect to that of δ free **L1**, Δδ being 0.71 ppm.

There are several reports on similar crystallographically characterized HgBr₂ • thione adducts in the literature such as [{BrHg(μ₂-Br)₂HgBr}(κ¹-methylimidazoline-2(3*H*)-thione)₂] (CSD refcode SUSWUY) and [{BrHg(μ₂-Br)₂HgBr}(κ¹-1,3-thiazolidine-2-thione)₂] (CSD refcode SUZCOF01).^[59,60] Both these thione complexes form dinuclear species, in which the two Hg centers are linked through two μ₂-bridging Br atoms. Furthermore, each tetrahedrally ligated Hg(II) center completes its coordination sphere with a terminal bromide ligand and a S-bonded

thione ligand. We therefore assume that complex **2a** shown in Scheme 3 is also dinuclear species [{BrHg(μ₂-Br)₂HgBr}(κ¹-**L1**)₂]. This hypothesis was confirmed by an X-ray diffraction study performed on single crystals of derivative [{BrHg(μ₂-Br)₂HgBr}(κ¹-**L2**)₂] **2b**, which was obtained in an identical manner by treatment of HgBr₂ with **L2** (Scheme 3). The molecular structure of this compound crystallizing in the triclinic space group $P\bar{1}$ is shown in Figure 7. Like the above cited HgBr₂ thione complexes, **2b** contains a dinuclear rhomboid-shaped Hg(μ₂-Br)₂Hg core, in which the two crystallographically different Hg nuclei are separated by 3.866 Å. A comparable loose contact of 3.901 Å, which is far from being considered as bonding (see structure of **1a**), was encountered in [{BrHg(μ₂-Br)₂HgBr}(κ¹-methylimidazoline-2(3*H*)-thione)₂].^[59] Each distorted tetrahedrally coordinated Hg atom [with angles values in the range between 87.368(19) and 147.30(2)°] is ligated by two rather symmetrically bridging μ₂-Br atoms and terminal bromido ligand. The coordination is completed by the **L2** ligand, which is bonded *via* its thione function. The mean Hg-S bond length is markedly longer than that of Cu compound **2a** [2.463(8) vs. 2.2561(4) Å], but matches approximately with that of [{BrHg(μ₂-Br)₂HgBr}(κ¹-methylimidazoline-2(3*H*)-thione)₂]

[2.406(4) Å]. The mean C=S bond length in **2b** is as expected somewhat elongated with respect to that of free **L2** [1.697(3) vs. 1.6593(10) Å]. The intermolecular H-bonding described for **L2** is also present in the solid-state structure of **2b** (Figure 7, bottom). Strong intermolecular N-H...O=P bonding gives rise to an infinite supramolecular 1D ribbon. As encountered for **1a**, the hydrogen bonding occurs through pairwise bridging of the N-H...O atoms forming 10-membered rings. The H1...O4 and H2...O1 contacts of 2.01(4) and 2.11(4) Å are slightly different and form N1-H1...O1 and N-H2...O1 angles of 150(4) and 163(4)°, respectively.

In a similar manner, heating a toluene solution of HgI₂ with an equimolar amount of **L2** for 15 min at 90° C produced upon cooling yellowish air-stable crystals of [{IHg(μ₂-I)₂HgI}(κ¹-**L2**)₂] **2c**. Based on elemental analysis and the crystal structure of **2b**, we suggested a similar architecture for **2c**, incorporating a dinuclear IHg(μ₂-I)₂HgI core (Scheme 3). Indeed, an X-ray diffraction confirmed this assumption. Figure 8 shows the molecular structure of this dimeric compound containing two crystallographically nonequivalent Hg atoms. The mean Hg-S bond length of 2.5794(7) Å is elongated compared with that of **2b**, indicating a somewhat weaker bonding of **L2** on Hg. In contrast, the mean C=S bond length of **2c** is slightly shortened with respect to that of free **2b** [1.689(3) vs. 1.697(3) Å]. A similar framework has been crystallographically established for [{IHg(μ₂-I)₂HgI}(κ¹-1,3-thiazolidine-2-thione)₂] (CSD refcode UHABEK) and [{IHg(μ₂-I)₂HgI}(κ¹-1,3-dimethyl-1,3-dihydro-2*H*-imidazole-2-thione)₂] (CSD refcode RIMKEG).^[60,61] An intermolecular H-bonding as encountered is also present in the solid-state structure of **2c** through N-H...O=P bonding. The resulting infinite supramolecular 1D ribbon is depicted in Figure S28. Again, the



Scheme 3. Synthesis of dinuclear complexes **2a–2c** and of the tetranuclear compound **3**.

hydrogen bonding occurs through pairwise bridging of the N–H···O atoms forming 10-membered rings. The H1···O4 and H2···O1 contacts of 1.92(3) and 1.96(3) Å are even below 2 Å and form N1–H1···O1 and N–H2···O1 angles of 148.3 and 145.7° respectively.

In order to isolate complex **2a** as the only product, it is advantageous to add **L1** in a 10% excess and to heat the mixture for at least 15–20 min. Otherwise, a colorless compound co-crystallizes, which has been identified by an X-ray diffraction study to be an unusual tetranuclear compound **3** of composition $[\text{Hg}_4\text{Br}_8(\kappa^1\text{-L1})_2]$, having a 2:1 HgBr_2 -to-**L1** ratio. This compound forms as major component in over 80% yield when using a 2:1 metal-to-ligand stoichiometry. The centrosymmetric molecular structure of $[\text{BrHg}(\kappa^1\text{-L1})(\mu_2\text{-Br})\{\text{BrHg}(\mu_2\text{-Br})_2\text{HgBr}\}(\mu_2\text{-Br})\text{HgBr}(\kappa^1\text{-L1})]$, which co-crystallized with one toluene molecule, is shown in Figure 9 and contains a $\{\text{BrHg}(\mu_2\text{-Br})_2\text{HgBr}\}$ core, which is interconnected further with two three-coordinate Hg1 atoms through Hg2–Br2–Hg1 bridges. Whereas the inner tetra-coordinate dinuclear Hg2 core contains exclusively terminal and bridging bromide ligands, the two terminal Hg1 atoms complete their coordination spheres by a dative $\text{Hg}\leftarrow\text{S}$ bonding *via* the thione function of **L2**. To avoid a lengthy structural discussion, all relevant Hg–Br bond length and distances are presented in the caption of Figure 9.

The Hg–S bond distance of **3** is shorter than that of **2b** [2.3818(11) vs. 2.463(8) Å], which may be indicative for a

stronger metal–ligand interaction. In consequence, the C=S bond length of **3** is slightly elongated with respect to that of **2b** [1.706(4) vs. 1.697(3) Å]. Noteworthy is also the occurrence of a weak incipient intramolecular hydrogen bonding within the almost planar C1–N1–H1···O1–P pseudo-cyclic array (see Figure 9 top). In contrast, **3** displays in the solid state strong intermolecular hydrogen bonds between the P=O groups of adjacent molecular units. As in the case of **1a**, due to this hydrogen bonding through pairwise bridging of the N–H···O1 atoms, 10-membered macrocycles are formed, which propagate along the *c* axis and give rise to a one-dimensional supramolecular metallopolymer. The H1···O1 contact of 2.005(3) Å is of the comparable strength as that of **1a**, with an N–H···O angle of 148.8(3)° (Figure 8 bottom).

This rare tetranuclear architecture has already been described for the pentaethylglycol-chelated compound $[\text{BrHg}(\text{peg})(\mu_2\text{-Br})\{\text{BrHg}(\mu_2\text{-Br})_2\text{HgBr}\}(\mu_2\text{-Br})\text{HgBr}(\text{peg})]$ (CSD refcode PODWOU) and the tetradentate Schiff-base compound $[\text{BrHg}(\text{bapm})(\mu_2\text{-Br})\{\text{BrHg}(\mu_2\text{-Br})_2\text{HgBr}\}(\mu_2\text{-Br})\text{HgBr}(\text{bapm})]$ (*bapm* = benzilbis((acetylpyridin-2-yl)methylidenehydrazone)) (CSD refcode KUCXAJ).^[62,63] But so far, no related organosulfur-ligated tetranuclear assembly has been described.

UV-vis and emission spectra

The UV-visible absorption spectra of **L1** and **L2** ligands recorded in acetonitrile exhibit a single band with maxima

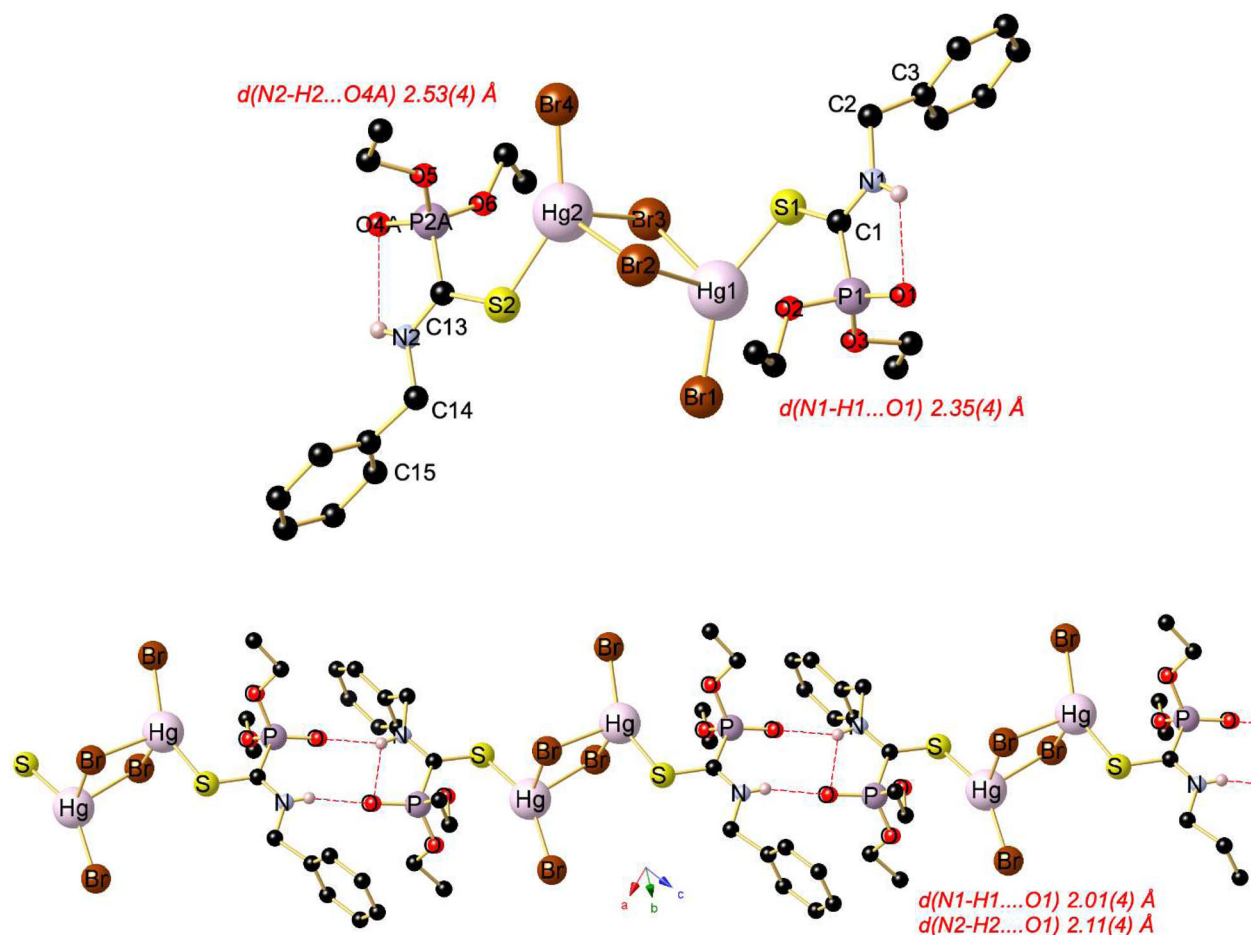


Figure 7. Molecular structure of **2b** in the crystal. Selected bond lengths (Å) and angles (deg): Hg1–Br1 2.4720(3), Hg1–Br2 2.7622(3), Hg1–Br31 2.8325(3), Br2–Hg2 2.8048(3), Hg1–S1 2.4445(8), Hg2–S2 2.4803(7), S1–C1 1.698(3), S2–C13 1.695(3), P1–O1 1.461(2), P1–O3 1.562(2), N1–C1 1.303(4), N1–C2 1.469(4), C2–C3 1.502(4), C3–C4 1.388(4); Br1–Hg1–Br2 104.961(12), Br1–Hg1–Br31 108.837(12), Br2–Hg1–Br31 89.918(9), Br3–Hg2–Br22 91.348(10), Br4–Hg2–Br3 105.752(12), Br4–Hg2–Br22 105.308(11), S1–Hg1–Br1 147.30(2), S1–Hg1–Br2 103.21(2), S1–Hg1–Br31 87.368(19), Hg1–Br2–Hg21 88.531(9), Hg2–Br3–Hg12 88.780(9), C1–S1–Hg1 108.52(11), C13–S2–Hg1 110.18(10), O1–P1–O2 118.81(15), C9–O2–P1 122.5(2), C11–O3–P1 118.6(2), S1–C1–P1 123.70(17), N1–C1–S1 122.8(2), N1–C1–P1 113.5(2). Symmetry transformations used to generate equivalent atoms: $^11+x, +y, -1+z$; $^2-1+x, +y, 1+z$. (Bottom) View of a segment of the supramolecular 1D ribbon of **2b**.

at 288 and 285 nm (Figure 10A), respectively. Substitution of cyclohexyl in **L1** ($\epsilon = 4700$) by benzyl **L2** ($\epsilon = 9400$) results in a notable increase of the molar extinction coefficient. Previous studies of the UV–vis absorption properties of thiocarbamoylphosphonates have shown that the spectra of this family of molecules exhibit two bands around 285 and 395 nm, assigned to $\pi \rightarrow \pi^*$ and $n \rightarrow \pi^*$ transitions.^[19] However, this latter attribution seems to be less likely in the case of our ligands because of its insensitivity to the change of the solvent polarity. Indeed, the absorption spectra measured for **L2** in hexane, ethanol and acetonitrile (Figure S29) exhibit all a similar appearance, which allows to attribute this band unambiguously to a $\pi \rightarrow \pi^*$ transition.

In contrast to the UV–vis spectrum of ligand **L1**, that of **1a** (Figure 10B) displays two bands at 288 nm attributed to ligand-centered transition and an additional band at 246 nm probably centered on the Cu_2I_2 fragment. The spectrum shape of complex **2a** is similar to that of **1a** (Figure 10B), but with a weak 4 nm bathochromic shift of the lower energy band centered on the ligand due to the heavy metal attractor effect. A second band at 233 nm is centered on the Hg_2Br_4 unit. In contrast, the absorption spectrum of complex **2c** (Figure 10C), shows a single band with a maximum

at 274 nm. In view of the increase in the width of this band at mid-height (~ 53 nm) compared to that of isostructural complex **2b** (~ 38 nm), the band observed for **2c** may be a mixture of transitions centered on **L2** and the Hg_2I_4 unit.

During this study we were also interested in the luminescence properties of the ligands and some complexes. After excitation at 300 nm, a weak emission band was observed for **L1** and **L2** (Figure 11A) with maxima at 397 and 401 nm, respectively. Upon excitation of solutions of complexes **1a** and **2b** using the same wavelength (Figure 11B), emission bands are observed displaying maxima at 379 and 364 nm (small Stokes shift), which are centered on ligands **L1** and **L2**, respectively. This study revealed that this emission bands are independent of the excitation wavelength. These fluorescence bands can be assigned to the lowest energy singlet state $S_1 \rightarrow S_0$ transition.

Conclusion and perspectives

We have reexamined in this contribution by two state-of-the-art X-ray diffraction studies at 100 K the interesting propensity of phosphonothioamidates to associate via strong

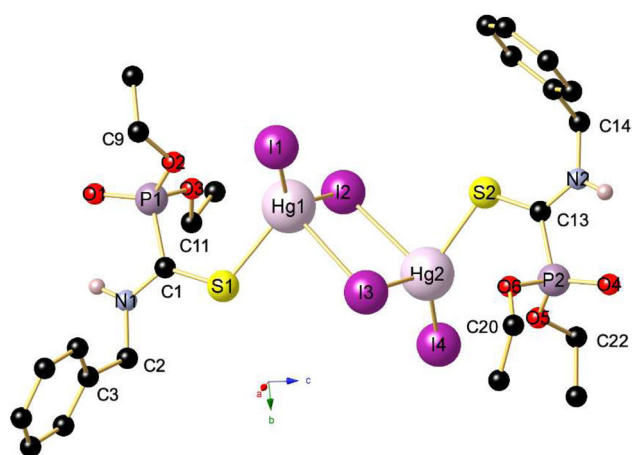


Figure 8. Molecular structure of **2c** in the crystal. Selected bond lengths (Å) and angles (deg): Hg1–I1 2.6687(3), Hg1–I2 2.7285(3), Hg1–I3 3.0987(3), Hg2–I2 3.1641(3), Hg2–I3 2.7613(3), Hg2–I4 2.6752(3), Hg1–S1 2.6106(7), Hg1–S2 2.5481(8), S1–C1 1.685(3), S2–C13 1.692(3), P1–O1 1.470(2), P1–O3 1.559(2), N1–C1 1.314(3), N1–C2 1.461(4), C2–C3 1.504(4), C3–C4 1.394(4); I1–Hg1–I2 133.272(8), I1–Hg1–I3 100.415(10), I2–Hg1–I3 93.694(8), I3–Hg2–I2 91.638(8), I4–Hg2–I2 103.885(9), I4–Hg2–I3 122.688(8), Hg1–I2–Hg2 86.816(7), Hg2–I3–Hg1 87.559(8), S1–Hg1–I1 117.050(19), S1–Hg1–I2 108.471(18), S2–Hg2–I2 86.287(18), S2–Hg2–I3 107.532(19), C1–S1–Hg1 112.56(10), C13–S2–Hg1 109.65(10), O1–P1–O2 116.68(14), C9–O2–P1 121.7(2), C11–O3–P1 120.0(2), S1–C1–P1 122.80(15), N1–C1–S1 124.1(2), N1–C1–P1 113.03(19).

intermolecular hydrogen bonding to yield both supramolecular dimers featuring 10-membered macrocycles (**L1** and **L2**) or one-dimensional chains (**L3**) and obtained more accurate crystallographic data sets. We have demonstrated for the first time that these compounds, known since more than 50 years, are also promising ligands in coordination chemistry. In the case of CuI, unusual low-coordinate dinuclear species $[\{\text{Cu}(\mu_2\text{-I})_2\text{Cu}\}(\kappa^1\text{-L})_2]$ are formed, which feature extremely short intermetallic Cu–Cu distances. A crystallographic analysis of **1a** also revealed, that the intrinsic propensity of thione-bonded **L** ligands allows the assembly of supramolecular metallopolymers. Dinuclear halide-bridged species $[\{\text{XHg}(\mu_2\text{-X})_2\text{HgX}\}(\kappa^1\text{-L})_2]$ without close metal–metal contact result also upon coordination on HgX_2 salts. Preliminary investigations indicated also that the variation of the metal-to-ligand ratio may also control the architecture and nuclearity of the coordination compound, as exemplified for the tetranuclear complex $[\text{Hg}_4\text{Br}_8(\kappa^1\text{-L1})_2]$ **3**. Apart from these structural features, Hg(II) thione complexes may also exhibit an antibacterial activity, as recently demonstrated for mercury imidazole-2-thione complexes.^[64] This may also represent one potential application for our compounds. In prospective work, we also intend to explore the coordination chemistry of **L1** and **L2** vis-à-vis other Cu(I) salts and harder paramagnetic CuX_2 salts to investigate their photophysical properties. Both systematic variation

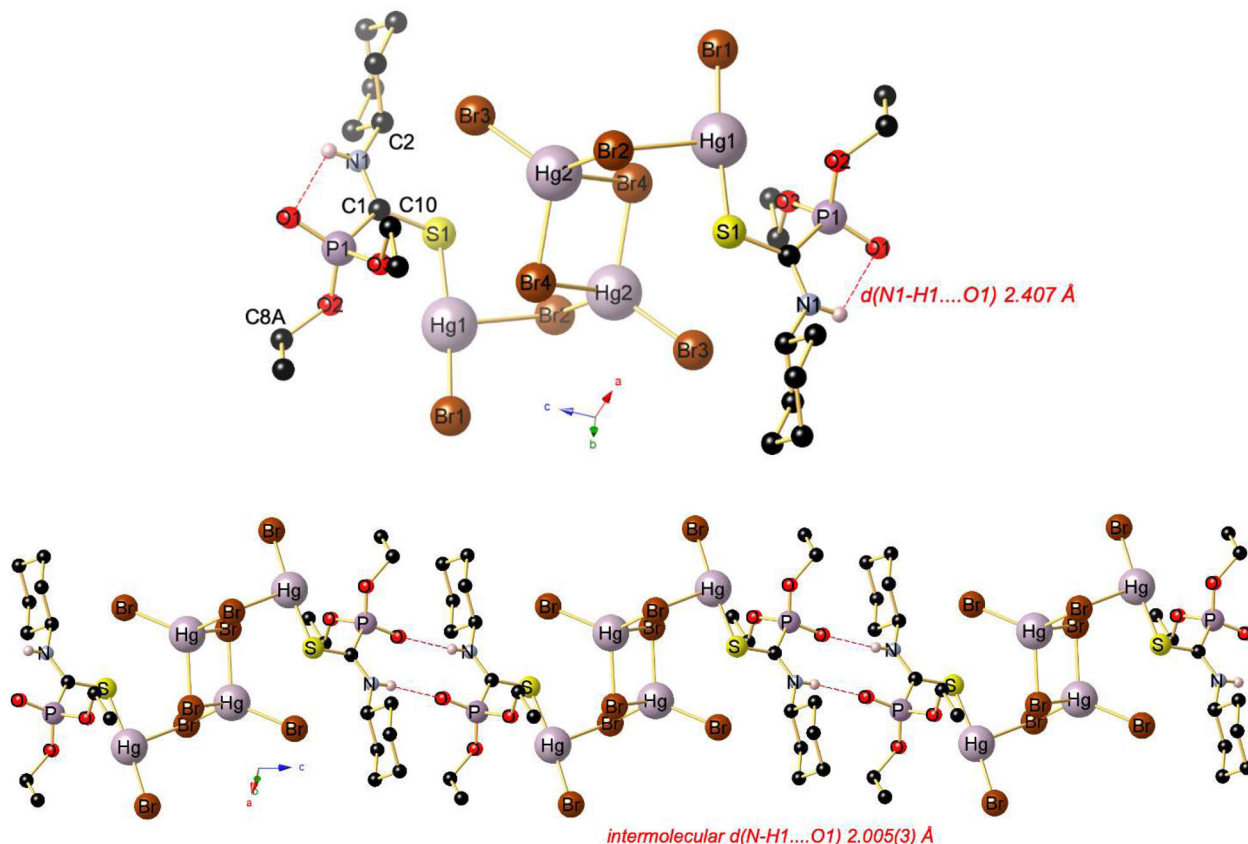


Figure 9. (Top) Molecular structure of **3** in the crystal. Selected bond lengths (Å) and angles (deg): Hg1–Br1 2.4241(7), Hg1–Br2 3.0554(6), Hg2–Br2 2.8325(3), Hg2–Br3 2.5128(5), Hg2–Br4 2.6884(6), Hg2–Br41 2.7938(5), Hg21–Br41 2.7937(5), Hg1–S1 2.3818(11), S1–C1 1.706(4), P1–O1 1.471(3), P1–O3 1.563(3), N1–C2 1.474(5), C2–C3 1.522(7), Hg2...Hg2 3.825; Br1–Hg1–Br2 106.69(2), S1–Hg1–Br1 173.57(3), S1–Hg1–Br2 79.74(3), Br2–Hg2–Br41 102.863(17), Br2–Hg2–Br4 107.759(18), Br3–Hg2–Br2 124.813(16), Br3–Hg2–Br41 108.961(17), Br3–Hg2–Br4 115.020(16), Br4–Hg2–Br41 91.516(18), Hg2–Br4–Hg21 88.486(18), C1–S1–Hg1 105.23(15), O1–P1–O2 119.09(18), O1–P1–C1 111.02(18), S1–C1–P1 123.4(2), N1–C1–S1 122.3(3), N1–C1–P1 114.3(3), N1–C2–C3 108.5(4), C3–C2–C7 111.9(4), C2–C7–C6 110.4(4). (Bottom) View of a segment of the supramolecular 1D ribbon of **3** running along the *c* axis. Symmetry transformations used to generate equivalent atoms: $1/2-x, 3/2-y, 1-z$; $2^1-x, +y, 3/2-z$.

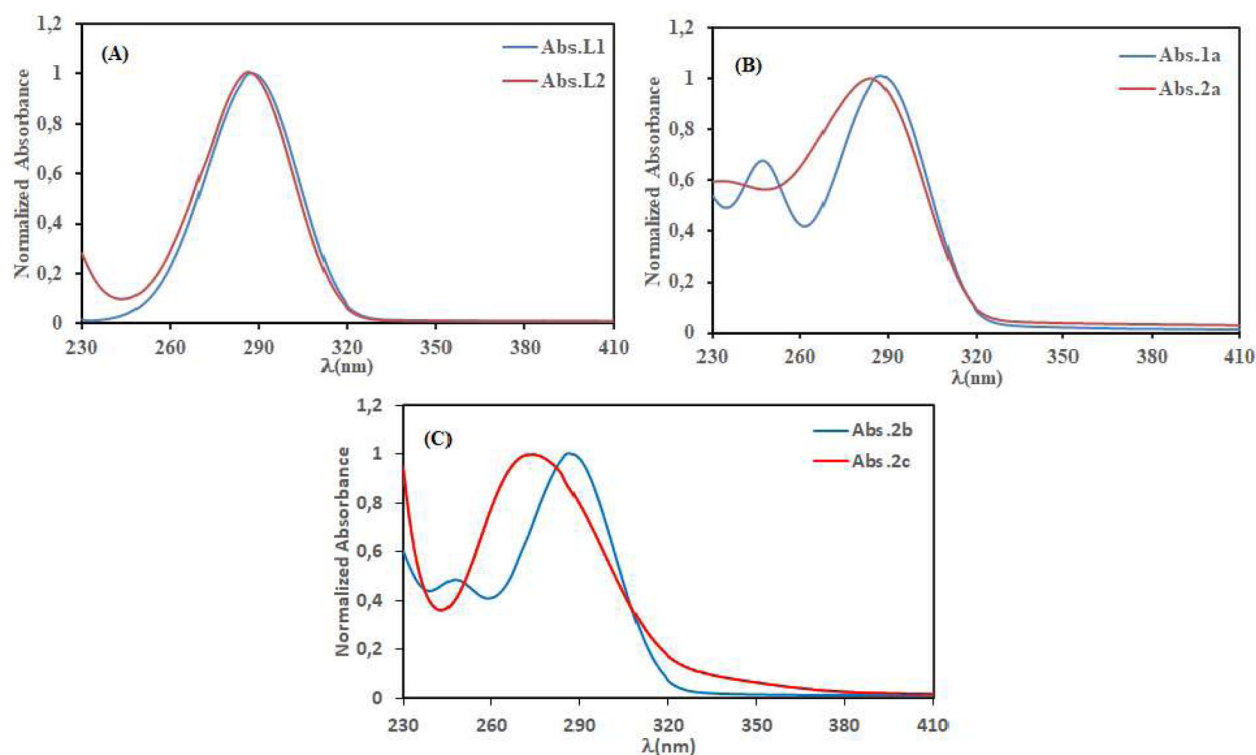


Figure 10. Normalized absorption spectra recorded in CH_3CN of ligands L1, L2 (A), complexes 1a, 2a (B) and 2b, 2c (C) at 298 K.

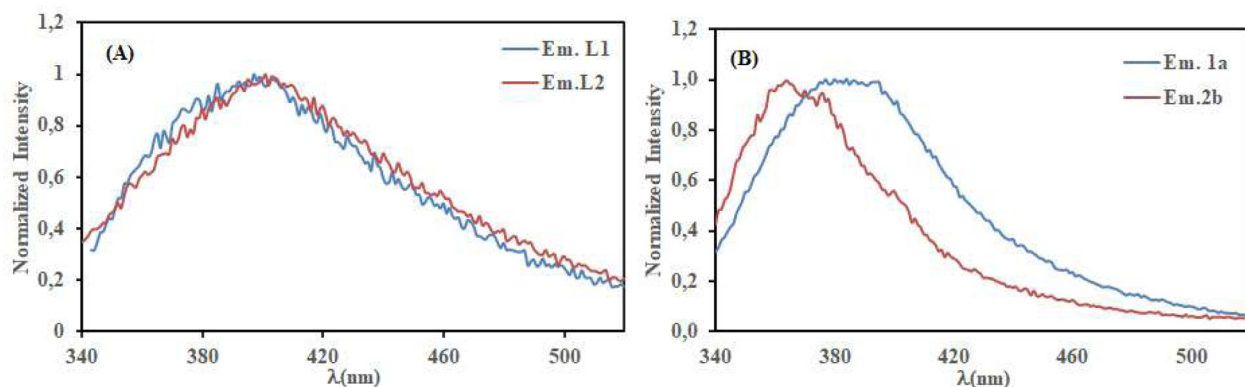


Figure 11. Normalized emission spectra recorded in CH_3CN of ligands L1, L2 (A) and complexes 1a, 2b (B) at 298 K.

of the metal-to-ligand ratio and the nature of the RO-substituents and N(H)-R groups will certainly impact the architecture of the complexes. Finally, the coordination chemistry of L toward harder metal complexes such as TiX_4 or ZrX_4 deserves future investigations to probe whether the $\text{P}=\text{O}$ function may interact with more oxophilic metal centers.

Experimental section

Apparatus

Infrared spectra have been obtained with a Shimadzu IR affinity-1 spectrometer using the ATR technique (germanium crystal). UV-vis spectra were measured with a VARIAN-Cary 100 spectrophotometer and emission spectra were recorded with a Jobin-Yvon FluoroLog 3.2.2 instrument in CH_3CN at room temperature. The ^1H , $^{13}\text{C}\{^1\text{H}\}$ and $^{31}\text{P}\{^1\text{H}\}$ NMR spectra were recorded with a Bruker

Avance 400 HD spectrometer operating at 400, 100 and 162 MHz, respectively. The Supplemental Materials contains sample of ^1H , ^{13}C , ^{31}P NMR and IR spectra of the products (Figures S1–S27).

General X-ray crystal structure analysis and refinement

The crystal structure determination was accomplished on a Bruker D8 Venture four-circle diffractometer using a PHOTON II CPAD detector by Bruker AXS GmbH. X-ray radiation was generated by microfocus source $\text{I}\mu\text{S}$ and $\text{I}\mu\text{S}$ 3.0 Mo ($\lambda = 0.71073 \text{ \AA}$) by Incoatec GmbH with HELIOS mirror optics and a single-hole collimator by Bruker AXS GmbH. Suitable crystals of L1, L2, 1a and 2b were covered with an inert oil (perfluoropolyalkylether) and mounted on a MicroMount from MiTeGen. For the data collection, the programs APEX 3 Suite (v.2018.7-2) with the integrated

programs SAINT (integration) and SADABS (adsorption correction) by *BrukerAXS GmbH* were used. The processing and finalization of the crystal structures was done with the program Olex2.^[65] The crystal structure was solved with the ShelXT structure solution program using Intrinsic Phasing and refined with the ShelXL refinement package using Least Squares minimization.^[66,67] The non-hydrogen atoms were refined anisotropically. The C-bonded H atoms were placed in geometrically calculated positions and each was assigned a fixed isotropic displacement parameter based on a riding model: C-H = 0.95–0.99 Å with $U_{\text{iso}}(\text{H}) = 1.5 U_{\text{eq}}(\text{CH}_3)$ and $1.2 U_{\text{eq}}(\text{CH}_2, \text{CH})$ for other hydrogen atoms. The N-bonded hydrogen atoms were located in the difference-Fourier-map and refined independently. For **L2** the disorder of the ethyl group attached to O3 was split into two parts and refined with free variables, which results in an occupancy of 47:53. The disorder in **1a** was split and refined with free variables as well, which results in an occupancy of 71:29 for the positional disorder of the ethyl group attached to O2. In **2b**, a positional disorder of the phosphate, attached to C13, occurs. It was split into two parts and refined with free variables including the atoms P2, C23 and C24. The refinement results in an occupancy of 58:42.

The crystallographic data and structure refinement data for all compounds are contained in Tables S1–S2 (Supplemental Materials). Crystallographic data for the structures of **L1**, **L2**, **1a**, **2b** and **3** have been deposited with the Cambridge Crystallographic Data Center as supplementary publication number 2058770–2058774, that of **2c** as 2063292. Copies of these data can be obtained, free of charge, on application to CCDC, 12 Union Road, Cambridge CB2 1EZ, UK, Fax: 144-(0)1223-336033 or e-mail: deposit@ccdc.cam.ac.uk

General procedure of preparation of ligands

Diethyl phosphite (0.020 mol, 1.0 equiv.) was added dropwise to a stirred solution of potassium *tert*-butoxide (0.025 mol, 1.5 equiv.) in dry THF (20 mL) at 0 °C over a period of 30 min. After 1 h stirring at room temperature, the appropriate isothiocyanate (0.020 mol, 1 equiv.) dissolved in dry THF (5 mL) was added to the resulting solution and then stirred for 3 h. 20 mL of solution of H⁺/H₂O were added to a stirred solution and the mixture was extracted with dichloromethane (3 × 50 mL). The recombined organic layers were dried with anhydrous sodium sulfate, filtered and then concentrated. The residual oil was purified by silica gel column chromatography, using a hexane/ether (1:1) mixture as eluent to yield the pure products as yellow solids.

Diethyl N-cyclohexylcarbamothioylphosphonate (L1)

C₁₁H₂₂NO₃PS (MW = 279 g mol⁻¹). Yield: 80%. ¹H NMR (CDCl₃): δ = 1.15–1.24 (m, 2H, H_{cy}), 1.30 (t, $J_{\text{HP}} = 7.1$ Hz, 6H, CH₃), 1.36–2.01 (m, 8H, H_{cy}), 4.09–4.25 (m, 4H, CH₂O), 4.22–4.32 (m, 1H, H_{ipso} (C₆H₁₁)), 8.76 (br, 1H, NH). ¹³C{¹H} NMR (CDCl₃): δ = 16.2 (d, $J_{\text{CP}} = 6.3$ Hz, C9), 24.5 (C₆H₁₁-C), 25.3 (C₆H₁₁-C), 30.1 (C₆H₁₁-C), 53.7 (d, $J_{\text{CP}} = 7.7$ Hz, C2), 65.1 (d, $J_{\text{CP}} = 6.8$ Hz, C8), 192.2 (d, $J_{\text{CP}} = 179.1$ Hz, C1). ³¹P{¹H} NMR (CDCl₃): δ = -0.03. IR-ATR

(cm⁻¹): 1016 ν(-P-O-C-), 1161 ν(C=S), 1230 ν(P=O), 1442 ν(C-N), 2857; 2930; 2983 ν(C-H), 3175 ν(N-H).

Diethyl N-benzylthiocarbamoylphosphonate (L2)

C₁₂H₁₈NO₃PS (MW = 287.30 g mol⁻¹). Yield: 85%. ¹H NMR (CDCl₃): δ = 1.29 (t, $J_{\text{HP}} = 7.1$ Hz, 6H, CH₃), 4.09–4.26 (m, 4H, CH₂O), 4.78 (dd, $J_{\text{HP}} = 5.4$; 2.0 Hz, 2H, CH₂), 7.09–7.35 (m, 5H, Harom), 9.13 (br, 1H, NH). ¹³C{¹H} NMR (CDCl₃): δ = 16.2 (d, $J_{\text{CP}} = 6.4$ Hz, C10), 49.3 (d, $J_{\text{CP}} = 8.5$ Hz, C1), 65.1 (d, $J_{\text{CP}} = 6.8$ Hz, C9), 128.4 (d, $J_{\text{CP}} = 10.0$ Hz, C2), 129.0 (Ar-C), 135.1 (Ar-C), 193.2 (d, $J_{\text{CP}} = 180.5$ Hz, C8). ³¹P{¹H} NMR (CDCl₃): δ = 0.00. IR-ATR (cm⁻¹): 1021 ν(-P-O-C-), 1164 ν(C=S), 1238 ν(P=O), 1454 ν(C-N), 2929; 2979 ν(C-H), 3209 ν(N-H).

General procedure for the preparation of complexes 1a,b

Complex 1a

This compound was prepared as by mixing **L1** (279 mg, 1.0 mmol), dissolved in 2 mL of MeCN and CuI (190 mg, 1.0 mmol) in 5 mL of MeCN. After stirring overnight at ambient temperature, the solvent was allowed to evaporate partially. Yellowish crystals of **1a** suitable for X-ray diffraction were formed within several days and then collected by filtration. Yield: 90%, m.p.: 125 °C. Anal. Calcd. for C₂₂H₄₄Cu₂I₂N₂O₆P₂S₂ (MW = 939.53 g mol⁻¹): C, 28.12; H, 4.72; N, 2.98; S, 6.82%; Found: C, 30.26; H, 5.02; N, 3.06; S, 6.55%. ¹H NMR (CD₃CN): δ = 0.83–2.40 (m, 16H, H_{cy}, CH₃), 3.88–4.31 (m, 4H, CH₂O), 4.31–4.86 (m, 1H, H_{ipso} (C₆H₁₁)), 9.16 (s, 1H, NH). ¹³C{¹H} NMR (CD₃CN): δ = 16.1 (d, $J_{\text{CP}} = 6.0$ Hz), 25.0, 25.6, 30.7, 54.5 (d, $J_{\text{CP}} = 7.5$ Hz), 64.1 (d, $J_{\text{CP}} = 6.6$ Hz), 192.3 (d, $J_{\text{CP}} = 181.0$ Hz, C=S). ³¹P{¹H} NMR (CD₃CN): δ = -1.4. IR-ATR (cm⁻¹): 668 σ(C-S), 1004 ν(-P-O-C-), 1156 ν(C=S), 1240 ν(P=O), 1447 ν(C-N), 2855; 2933 ν(C-H), 3014 ν(N-H...O), 3151 ν(N-H).

Complex 1b

This compound was prepared as described above from **L2** (58 mg, 0.2 mmol) and CuI (48 mg, 0.2 mmol) using 3 mL of MeCN. Yield: 79%. Anal. Calcd. for C₂₅H₃₉Cu₂I₂N₂O₆P₂S₂ (MW = 970.56 g mol⁻¹): C, 30.94; H, 4.05; N, 2.89; S, 6.61%; Found: C, 33.04; H, 4.35; N, 2.97; S, 6.48%. ¹H NMR (CD₃CN): δ = 1.32 (t, $J = 7.0$ Hz, 6H, CH₃), 3.85–4.43 (m, 4H, OCH₂), 4.93 (s, 2H, CH₂), 7.11–7.67 (m, 5H, H_{arom}), 9.78 (s, 1H, NH). ³¹P{¹H} NMR (CD₃CN): δ = -1.6. IR-ATR (cm⁻¹): 694 ν(C-S), 1020 ν(-P-O-C-), 1161 ν(C=S), 1239 ν(P=O), 1451 ν(C-N), 2932; 2978 ν(C-H), 3210 ν(N-H).

General procedure for the preparation of complexes 2a–c

To a solution of HgX₂ (X = Br, I; 1 mmol) in toluene (9 mL) was added 1 equiv. of **L**. The mixture was heated to 90 °C

for 15 min and then allowed to reach slowly ambient temperature. After one day, yellowish crystals of **2a–c** were formed (suitable for X-ray diffraction in the case of **2b** and **2c**) and filtered off.

Complex 2a

This compound was prepared as described above from **L1** (139.5 mg, 0.5 mmol) and HgBr₂ (180 mg, 0.5 mmol). Yield: 73%. Anal. Calcd. for C₂₂H₄₄Br₄Hg₂N₂O₆P₂S₂ (MW = 1279.48 g mol⁻¹): C, 20.65; H, 3.47; N, 2.19; S, 5.01%; Found: C, 20.37; H, 3.15; N, 1.98; S, 4.81%. ¹H NMR (CD₃CN): δ = 1.21–1.33 (m, 2H, H_{CY}), 1.36 (t, J_{HP} = 7.1 Hz, 6H, CH₃), 1.47 (dd, J = 25.3, 13.7 Hz, 4H, H_{CY}), 1.69 (d, J = 12.9 Hz, 1H, H_{CY}), 1.82 (d, J = 12.9 Hz, 2H, H_{CY}), 2.01 (dd, J = 12.5, J = 2.2 Hz, 2H, H_{CY}), 4.19–4.34 (m, 4H, CH₂O), 4.39 (s, 1H, H_{ipso}(C₆H₁₁)), 9.48 (s, 1H, NH). ³¹P{¹H} NMR (CD₃CN): δ = 1.25. IR-ATR (cm⁻¹): 796 σ(C–S), 1009 ν(–P–O–C–), 1157 ν(C=S), 1238 ν(P=O), 1469 ν(C–N), 2856; 2932; 2982 ν(C–H), 3112 ν(N–H).

Complex 2b

This compound was prepared as described above from **L2** (143.5 mg, 0.5 mmol) and HgBr₂ (180 mg, 0.5 mmol). Yield: 78% m.p.: 132 °C. Anal. Calcd. for C₂₄H₃₆Br₄Hg₂N₂O₆P₂S₂ (MW = 1295.43 g mol⁻¹): C, 22.25; H, 2.80; N, 2.16; S, 4.95% Found: C, 26.87; H, 3.35; N, 2.55; S, 5.51%. ¹H NMR (CD₃CN): δ = 1.32 (t, J_{HP} = 7.1 Hz, 6H, CH₃), 4.28–4.09 (m, 4H, CH₂O), 4.93 (s, 2H, CH₂), 7.44–7.28 (m, 5H, H_{arom}), 9.84 (s, 1H, NH). ¹³C{¹H} NMR (CD₃CN): δ = 16.1 (d, J_{CP} = 6.1 Hz), 48.3 (d, J_{CP} = 8.6 Hz), 65.0 (d, J_{CP} = 6.7 Hz), 128.1 (Ar–C), 128.4 (Ar–C), 129.1 (Ar–C), 136.8 (Ar–C), 194.6 (d, J_{CP} = 182 Hz, C=S). ³¹P{¹H} NMR (CD₃CN): δ = –1.6. IR-ATR (cm⁻¹): 692 σ(C–S), 1008 ν(–P–O–C–), 1162 ν(C=S), 1237 ν(P=O), 1442 ν(C–N), 2930 ν(C–H), 3209 ν(N–H).

Complex 2c

This compound was prepared as described above mixing **L2** (28.3 mg, 0.1 mmol) and HgI₂ (45.4 mg, 0.1 mmol) in 2 mL of hot toluene. Yield: 73%. Anal. Calcd. for C₂₄H₃₆Hg₂I₄N₂O₆P₂S₂ (MW = 1419.44 g mol⁻¹): C, 20.30; H, 2.56; N, 1.97; S, 4.52% Found: C, 20.77; H, 2.85; N, 1.65; S, 4.21%. ¹H NMR (d₆-DMSO, 333 K): δ = 1.25 (t, ³J_{HP} = 7.0 Hz, 6H, CH₃), 3.96–4.19 (m, 4H, CH₂O), 4.82 (s, 2H, CH₂), 7.09–7.54 (m, 5H, H_{arom}), 11.23 (s, 1H, NH). ³¹P{¹H} NMR (d₆-DMSO): δ = –0.85. IR-ATR (cm⁻¹): 694 σ(C–S), 1021 ν(–P–O–C–), 1158 ν(C=S), 1246 ν(P=O), 1439 ν(C–N), 2962 ν(C–H), 3120 ν(N–H⋯O), 3204 ν(N–H).

Complex 3

This compound was prepared by reaction of **L1** (70 mg, 0.25 mmol) with two equiv. of HgBr₂ (180 mg, 0.5 mmol) at 100 °C. Yield: 47%. Anal. Calcd. for C₂₉H₅₃Br₈Hg₄N₂O₆P₂S₂ (MW = 2093.43 g mol⁻¹): C, 13.76; H, 2.31; N, 1.46; S, 3.34%; Found: C, 14.25; H, 2.22; N, 1.62; S, 3.04%. ¹H NMR

(d₆-DMSO, 333 K): δ = 1.12–1.24 (m, 3H, H_{CY}), 1.27 (t, J = 7.0 Hz, 6H, CH₃), 1.46 (dd, J = 12.2 Hz, J = 3.1 Hz, 1H, H_{CY}), 1.52 (dd, J = 12.2 Hz, J = 3.4 Hz, 1H, H_{CY}), 4.05–4.21 (m, 4H, CH₂O), 4.14–4.40 (m, 1H, H_{ipso}(C₆H₁₁)), 10.16 (s, 1H, NH). ³¹P{¹H} NMR (d₆-DMSO): δ = –1.4. IR-ATR (cm⁻¹): 653 σ(C–S), 1003 ν(–P–O–C–), 1159 ν(C=S), 1254 ν(P=O), 1447 ν(C–N), 2852; 2933; 2984 ν(C–H), 3136 ν(NH⋯O), 3206 ν(N–H).

Acknowledgments

This work was supported by the Ministry of higher education and scientific research of Tunisia and by the CNRS. We thank Ms. Stephanie Boullanger for recording the NMR and ATR-IR spectra. L. B. thanks the Fonds der Chemischen Industrie (FCI) for a Chemiefonds Fellowship.

ORCID

Wafa Arar  <http://orcid.org/0000-0001-8669-2359>
 Abderrahim Khatyr  <http://orcid.org/0000-0003-4510-4412>
 Michael Knorr  <http://orcid.org/0000-0002-5647-8084>
 Lukas Brieger  <http://orcid.org/0000-0001-8462-7190>
 Anna Krupp  <http://orcid.org/0000-0002-5795-1830>
 Carsten Strohmann  <http://orcid.org/0000-0002-4787-2135>
 Mohamed Lotfi Efrif  <http://orcid.org/0000-0002-6950-0519>
 Azaiez Ben Akacha  <http://orcid.org/0000-0003-0171-2088>

References

- Masakatsu, S.; Motomu, K. Multifunctional Asymmetric Catalysis. *Chem. Pharm. Bull.* **2001**, *49*, 511–524. DOI: [10.1248/cpb.49.511](https://doi.org/10.1248/cpb.49.511).
- Schug, K. A.; Lindner, W. Noncovalent Binding between Guanidinium and Anionic Groups: Focus on Biological- And Synthetic-Based Arginine/Guanidinium Interactions with Phosph[on]Ate and Sulf[on]Ate Residues. *Chem. Rev.* **2005**, *105*, 67–113. DOI: [10.1021/cr040603j](https://doi.org/10.1021/cr040603j).
- Lerner, R. A.; Benkovic, S. J.; Schultz, P. G. At the Crossroads of Chemistry and Immunology: Catalytic Antibodies. *Science* **1991**, *252*, 659–667. DOI: [10.1126/science.2024118](https://doi.org/10.1126/science.2024118).
- Moonen, K.; Laureyn, I.; Stevens, C. V. Synthetic Methods for Azaheterocyclic Phosphonates and Their Biological Activity. *Chem. Rev.* **2004**, *104*, 6177–6215. DOI: [10.1021/cr030451c](https://doi.org/10.1021/cr030451c).
- Jackson, S. N.; Moyer, S. C.; Woods, A. S. The Role of Phosphorylated Residues in Peptide–Peptide Noncovalent Complexes Formation. *Am. Soc. Mass Spectrom.* **2008**, *19*, 1535–1541. DOI: [10.1016/j.jasms.2008.06.023](https://doi.org/10.1016/j.jasms.2008.06.023).
- Farkas, E.; Katz, Y.; Bhusare, S.; Reich, R.; Rösenthaler, G. V.; Königsmann, M.; Breuer, E. Carbamoylphosphonate-Based Matrix Metalloproteinase Inhibitor Metal Complexes: Solution Studies and Stability Constants towards a Zinc-Selective Binding Group. *J. Biol. Inorg. Chem.* **2004**, *9*, 307–315. DOI: [10.1007/s00775-004-0524-5](https://doi.org/10.1007/s00775-004-0524-5).
- Cermak, D. M.; Du, Y.; Wiemer, D. F. Synthesis of Nonracemic Dimethyl α-(Hydroxyfarnesyl) Phosphonates via Oxidation of Dimethyl Farnesylphosphonate with (Camphorsulfonyl)-Oxaziridines. *J. Org. Chem.* **1999**, *64*, 388–393. DOI: [10.1021/jo980984z](https://doi.org/10.1021/jo980984z).
- Breuer, E.; Katz, Y.; Hadar, R.; Reich, R. Carbamoylphosphonate MMP Inhibitors. Part 4: The Influence of Chirality and Geometrical Isomerism on the Potency and Selectivity of Inhibition. *Tetrahedron. Asymm.* **2004**, *15*, 2415–2420. DOI: [10.1016/j.tetasy.2004.07.002](https://doi.org/10.1016/j.tetasy.2004.07.002).
- Bilenko, V.; Spannenberg, A.; Baumann, W.; Komarov, I.; Börner, A. New Chiral Monodentate Phospholane Ligands by

- Highly Stereoselective Hydrophosphination. *Tetrahedr. Asymm.* **2006**, *17*, 2082–2087. DOI: [10.1016/j.tetasy.2006.06.047](https://doi.org/10.1016/j.tetasy.2006.06.047).
- [10] Rao, D. S.; Madhava, G.; Rasheed, S.; Thahir Basha, S.; Lakshmi Devamma, M. N.; Naga Raju, C. CeCl₃·7H₂O-SiO₂ Catalyzed Ultrasonicated Solvent-Free Synthesis of Carbamoyl/Carbamothioylphosphonates and Antimicrobial Activity Evaluation. *Phosphorus Sulfur Silicon Relat. Elem.* **2015**, *190*, 574–584. DOI: [10.1080/10426507.2014.974749](https://doi.org/10.1080/10426507.2014.974749).
- [11] Omrani, R.; Ben Ali, R.; Selmi, W.; Arfaoui, Y.; Véronique El May, M.; Ben Akacha, A. Synthesis, Design, DFT Modeling, Hirshfeld Surface Analysis, Crystal Structure, Anti-Oxidant Capacity and Anti-Nociceptive Activity of Dimethylphenylcarbamothioylphosphonate. *J. Mol. Struct.* **2020**, *1217*, 128429. DOI: [10.1016/j.molstruc.2020.128429](https://doi.org/10.1016/j.molstruc.2020.128429).
- [12] Tischer, T.; Goldmann, A. S.; Linkert, K.; Trouillet, V.; Börner, H. G.; Barner-Kowollik, C. Modular Ligation of Thioamide Functional Peptides onto Solid Cellulose Substrates. *Adv. Funct. Mater.* **2012**, *22*, 3853–3864. DOI: [10.1002/adfm.201200266](https://doi.org/10.1002/adfm.201200266).
- [13] Tashma, Z. N-Alkylthiocarbamoyl)Thionophosphonic Acid Esters. *J. Org. Chem.* **1983**, *48*, 3966–3969. DOI: [10.1021/jo00170a018](https://doi.org/10.1021/jo00170a018).
- [14] Tashma, Z. N-Alkyl Thiocarbonyl Phosphonic Acid Esters-2-Alkylation by Methyl Iodide Accompanied by Phosphonate Dealkylation. *Tetrahedron* **1982**, *38*, 3745–3747. DOI: [10.1016/0040-4020\(82\)80086-0](https://doi.org/10.1016/0040-4020(82)80086-0).
- [15] Young, R. C.; Robin Ganellin, C.; Graham, M. J.; Mitchell, R. C.; Roantree, M. L.; Tashma, Z. Zwitterionic Analogues of Cimetidine as H₂ Receptor Antagonists. *J. Med. Chem.* **1987**, *30*, 1150–1156. DOI: [10.1021/jm00390a006](https://doi.org/10.1021/jm00390a006).
- [16] Tashma, Z. N-Alkyl(Thio)Carbamoylphosphonic Acid Esters, Part 4. Inconsistent Solvent Shifts Caused by Benzene in the NMR Spectra of N-Alkyl(Thio)Phosphonothioamides. *Magn. Reson. Chem.* **1985**, *23*, 289–291. DOI: [10.1002/mrc.1260230502](https://doi.org/10.1002/mrc.1260230502).
- [17] Omrani, R.; Ben Amor, F.; Bahri, M.; Efrat, M. L.; Ben Akacha, A. Synthesis and Structural Studies of Phosphonothioamides. *Phosphorus Sulfur Silicon Relat. Elem.* **2015**, *190*, 1715–1726. DOI: [10.1080/10426507.2015.1024783](https://doi.org/10.1080/10426507.2015.1024783).
- [18] Omrani, R.; Efrat, M. L.; Ben Akacha, A. Reactivity of Phosphonothioamides with Acid Chlorides and Primary Amines: Synthesis and Conformational Study of N-Acylated Phosphonothioamides and Phosphonoamidines. *Phosphorus Sulfur Silicon Relat. Elem.* **2015**, *190*, 2291–2301. DOI: [10.1080/10426507.2015.1071372](https://doi.org/10.1080/10426507.2015.1071372).
- [19] Tashma, Z. (N-Alkylthiocarbamoyl)Phosphonic Acid Esters. I. Preparation and Spectral Properties. *J. Org. Chem.* **1982**, *47*, 3012–3015. DOI: [10.1021/jo00136a044](https://doi.org/10.1021/jo00136a044).
- [20] Lebouc, F.; Dez, I.; Gulea, M.; Madec, P. J.; Jaffrès, P. A. Synthesis of Phosphorus-Containing Chitosan Derivatives. *Phosphorus Sulfur Silicon Relat. Elem.* **2009**, *184*, 872–889. DOI: [10.1080/10426500802715585](https://doi.org/10.1080/10426500802715585).
- [21] Makomo, H.; Masson, S.; Saquet, M. Catalyzed Amination of Dithioacid Sodium Salts: A One Pot Synthesis of α -Phosphonothioamides. *Phosphorus Sulfur Silicon Relat. Elem.* **1993**, *80*, 31–36. DOI: [10.1080/10426509308036874](https://doi.org/10.1080/10426509308036874).
- [22] Morita, H.; Tashiro, S.; Takeda, M.; Yamada, N.; Chanmiya Sheikh, M. D.; Kawaguchi, H. The Reaction of Benzothiazolyl Substituted α -Phosphorylmethyl Sulfoxides with Several Amines. *Tetrahedron* **2008**, *64*, 4496–4505. DOI: [10.1016/j.tet.2008.02.028](https://doi.org/10.1016/j.tet.2008.02.028).
- [23] Roy-Gourvenec, S. L.; Lemarie, M.; Masson, S. Desulfurisation of Phosphonylated Thioamides: A New Way to Functionalised Aminophosphonates. *Phosphorus Sulfur Silicon Relat. Elem.* **1997**, *123*, 247–254. DOI: [10.1080/10426509708044213](https://doi.org/10.1080/10426509708044213).
- [24] Morita, H.; Tashiro, S.; Takeda, M.; Fujimori, K.; Yamada, N.; Chanmiya Sheikh, M.; Kawaguchi, H. Thermolyses of α -Phosphorylmethyl Tetrazolyl Sulfoxides in the Presence of 2,3-Dimethyl-1,3-Butadiene and Their Reactions with Several Amines. *Tetrahedron* **2008**, *64*, 3589–3595. DOI: [10.1016/j.tet.2008.01.082](https://doi.org/10.1016/j.tet.2008.01.082).
- [25] Reetz, T.; Chadwick, D. H.; Hardy, E. E.; Kaufman, S. Carbamoylphosphonates. *J. Am. Chem. Soc.* **1955**, *77*, 3813–3816. DOI: [10.1021/ja01619a040](https://doi.org/10.1021/ja01619a040).
- [26] Bulpin, A.; Roy-Gourvenec, S. L.; Masson, S. The Amination of Phosphonodithioformates: A Preparation of New Functionalised Phosphonates. *Phosphorus Sulfur Silicon Relat. Elem.* **1994**, *89*, 119–132. DOI: [10.1080/10426509408020441](https://doi.org/10.1080/10426509408020441).
- [27] Kolodyazhnaya, A. O.; Kolodyazhnaya, O. O.; Kolodyazhnyi, O. I. An Efficient Method for the Phosphonation of C=X Compounds. *Russ. J. Gen. Chem.* **2010**, *80*, 549–562. DOI: [10.1134/S1070363210040055](https://doi.org/10.1134/S1070363210040055).
- [28] Tieqiao, C.; Ji-Shu, Z.; Li-Biao, H. For Related Literature on the Transformation of P(=O)-H Compounds See References 28–31. Dehydrogenative Coupling Involving P(O)-H Bonds: A Powerful Way for the Preparation of Phosphoryl Compounds. *Dalton Trans.* **2016**, *45*, 1843–1849. DOI: [10.1039/C5DT01896J](https://doi.org/10.1039/C5DT01896J).
- [29] Tanveer Mahamadali, S.; Chia-Ming, W.; Fung-E. H. Secondary Phosphine Oxides: Versatile Ligands in Transition Metal-Catalyzed Cross-Coupling Reactions. *Coord. Chem. Rev.* **2012**, *256*, 771–803. DOI: [10.1016/j.ccr.2011.11.007](https://doi.org/10.1016/j.ccr.2011.11.007).
- [30] Chen, T.; Han, L.-B. Optically Active H-Phosphinates and Their Stereospecific Transformations into Optically Active P-Stereogenic Organophosphoryl Compounds. *Synlett.* **2015**, *26*, 1153–1163. DOI: [10.1055/s-0034-1379996](https://doi.org/10.1055/s-0034-1379996).
- [31] Chen, T.; Tan, Q.; Liu, X.; Liu, L.; Huang, T.; Han, L.-B. Phosphorylation of Carboxylic Acids and Their Derivatives with P(O)-H Compounds Forming P(O)-C Bonds. *Synthesis* **2021**, *53*, 95–106. DOI: [10.1055/s-0040-1707286](https://doi.org/10.1055/s-0040-1707286).
- [32] Kaboudin, B.; Zahedi, H. A Novel and Convenient Method for Synthesis of Carbamoyl and Thiocarbamoyl Phosphonates. *Synroatom Chem.* **2009**, *20*, 250–253. DOI: [10.1002/hc.20538](https://doi.org/10.1002/hc.20538).
- [33] Kolodiazhnyi, O. I.; Kolodiazhna, O. O. New Catalyst for Phosphonylation of C=X Electrophiles. *Synth. Commun.* **2012**, *42*, 1637–1649. DOI: [10.1080/00397911.2010.542602](https://doi.org/10.1080/00397911.2010.542602).
- [34] Tashma, Z.; Cohen, S. N-Alkylthiocarbamoylphosphonic Acid Esters. 5. Dimerization through a Ten-Membered Hydrogen-Bonded Ring. *Phosphorus Sulfur Silicon Relat. Elem.* **1985**, *22*, 357–363. DOI: [10.1080/03086648508073375](https://doi.org/10.1080/03086648508073375).
- [35] Pearson, R. G. Recent Advances in the Concept of Hard and Soft Acids and Bases. *J. Chem. Educ.* **1987**, *64*, 561–567. DOI: [10.1021/ed064p561](https://doi.org/10.1021/ed064p561).
- [36] Spackman, M. A.; Jayatilaka, D. Hirshfeld Surface Analysis. *CrytEngComm* **2009**, *11*, 19–32. DOI: [10.1039/B818330A](https://doi.org/10.1039/B818330A).
- [37] Turner, M. J.; McKinnon, J. J.; Wolff, S. K.; Grimwood, D. J.; Spackman, P. R.; Jayatilaka, D.; Spackman, M. A. University of Western Australia, **2017**.
- [38] Hameau, A.; Guyon, F.; Knorr, M.; Enescu, M.; Strohmman, C. Self-Assembly of Dithiolene-Based Coordination Polymers of Mercury(II): Dithioether Versus Thiocarbonyl Bonding. *Monatsh. Chem.* **2006**, *137*, 545–555. DOI: [10.1007/s00706-006-0449-5](https://doi.org/10.1007/s00706-006-0449-5).
- [39] Guyon, F.; Hameau, A.; Khatyr, A.; Knorr, M.; Amrouche, H.; Fortin, D.; Harvey, P. D.; Strohmman, C.; Ndiaye, A. L.; Huch, V. Syntheses, Structures, and Photophysical Properties of Mono- and Dinuclear Sulfur-Rich Gold(I) Complexes. *Inorg. Chem.* **2008**, *47*, 7483–7492. DOI: [10.1021/ic7022067](https://doi.org/10.1021/ic7022067).
- [40] Hameau, A.; Guyon, F.; Khatyr, A.; Knorr, M.; Strohmman, C. 4,5-Bis(Methylthio)-1,3-Dithiole-2-Thione, a Versatile Sulphur-Rich Building Block for the Self-Assembly of Cu(I) and Ag(I) Coordination Polymers: Dithioether Versus Thiocarbonyl Bonding. *Inorg. Chim. Acta* **2012**, *388*, 60–70. DOI: [10.1016/j.ica.2012.02.032](https://doi.org/10.1016/j.ica.2012.02.032).
- [41] Akvivos, P. D.; Kapsomenos, G.; Karagiannidis, P.; Skoulika, S.; Aubry, A. Preparation and Study of Three-Coordinate Mixed Ligand Copper(I) Compounds. Molecular and Crystal Structure of (Tricyclohexylphosphine)(2-Thioxohexamethyleneimine)Copper(I) iodide. *Inorg. Chim. Acta* **1992**, *202*, 73–77. DOI: [10.1016/S0020-1693\(00\)85353-0](https://doi.org/10.1016/S0020-1693(00)85353-0).
- [42] Yim, H. W.; Rabinovich, D.; Lam, K. C.; Golen, J. A.; Rheingold, A. L. Di- μ -Iodo-Bis{[Methyltris(Methylthiomethyl)

- Silane- k^2S,S' Copper(I)}. *Acta Crystallogr. E* **2003**, E59, m556–m558. DOI: [10.1107/S1600536803012947](https://doi.org/10.1107/S1600536803012947).
- [43] Olbrich, F.; Maelger, H.; Klar, G. Cyclic Ligands with Fixed Coordination Geometry. Part 8. Structure of $[CuCl(Vn_3S_3)] \cdot 2 THF$ and of $[CuCl(Me_2S)_3]$ for Comparison ($Vn_3S_3 = 5,10,15$ -Trithia-Cyclo-Triveratrylene). *Transition Met. Chem.* **1992**, 17, 525–529. DOI: [10.1007/BF02910749](https://doi.org/10.1007/BF02910749).
- [44] Henline, K. M.; Wang, C.; Pike, R. D.; Ahern, J. C.; Sousa, B.; Patterson, H. H.; Kerr, A. T.; Cahill, C. L. Structure, Dynamics, and Photophysics in the Copper(I) Iodide-Tetrahydrothiophene System. *Crystallogr. Growth Des.* **2014**, 14, 1449–1458. DOI: [10.1021/cg500005p](https://doi.org/10.1021/cg500005p).
- [45] Lapprand, A.; Bonnot, A.; Knorr, M.; Rousselin, Y.; Kubicki, M. M.; Fortin, D.; Harvey, P. D. Formation of an Unprecedented $(CuBr)_5$ Cluster and Zeolite-Type 2D-Coordination Polymer; A Surprising Halide Effect. *Chem. Commun.* **2013**, 49, 8848–8847. DOI: [10.1039/C3CC44183K](https://doi.org/10.1039/C3CC44183K).
- [46] Harvey, P. D.; Bonnot, A.; Lapprand, A.; Strohmman, C.; Knorr, M. Coordination $RC_6H_4S(CH_2)_8SC_6H_4R/(CuI)_n$ Polymers ($R(n)=H(4); Me(8)$): An Innocent Methyl Group That Makes the Difference. *Macromol. Rapid Commun.* **2015**, 36, 654–659. DOI: [10.1002/marc.201400659](https://doi.org/10.1002/marc.201400659).
- [47] Raghuvanshi, A.; Dargally, N. J.; Knorr, M.; Viau, L.; Knauer, L.; Strohmman, C. 1,3-Dithiolane and 1,3-Ferrocenyl-Dithiolane as Assembling Ligands for the Construction of Cu(I) Clusters and Coordination Polymers. *J. Inorg. Organomet. Polym.* **2017**, 27, 1501–1513. DOI: [10.1007/s10904-017-0610-0](https://doi.org/10.1007/s10904-017-0610-0).
- [48] Lobana, T. S.; Sharma, R.; Hundal, G.; Castineiras, A.; Butcher, R. J. The Influence of Substituents (R) at N^1 Atom of Furan-2-Carbaldehyde Thiosemicarbazones $\{(C_4H_3O)HC^2=N^3-N(H)-C^1(=S)N^1HR\}$ on Bonding, Nuclearity, H-Bonded Networks of Copper(I) Complexes. *Polyhedron* **2012**, 47, 134–142. DOI: [10.1016/j.poly.2012.08.014](https://doi.org/10.1016/j.poly.2012.08.014).
- [49] Lobana, T. S.; Butcher, R. J. Metal-Thiosemicarbazone Interactions. Synthesis of an Iodo-Bridged Dinuclear [Diodobis(Pyrrole-2-Carbaldehydethiosemicarbazone)Dicopper (I)] Complex. *Transit. Met. Chem.* **2004**, 29, 291–295. DOI: [10.1023/B:TMCH.0000020371.72284.4d](https://doi.org/10.1023/B:TMCH.0000020371.72284.4d).
- [50] Troyano, J.; Perles, J.; Amo-Ochoa, P.; Zamora, F.; Delgado, S. Strong Luminescent Copper(I) Halide Coordination Polymers and Dinuclear Complexes with Thioacetamide and N,N' -Donor Ligands. *CrystEngComm.* **2016**, 18, 1809–1817. DOI: [10.1039/C5CE02264A](https://doi.org/10.1039/C5CE02264A).
- [51] Troyano, J.; Zapata, E.; Perles, J.; Amo-Ochoa, P.; Fernández-Moreira, V.; Martínez, J. I.; Zamora, F.; Delgado, S. Multifunctional Copper(I) Coordination Polymers with Aromatic Mono- and Ditopic Thioamides. *Inorg. Chem.* **2019**, 58, 3290–3301. DOI: [10.1021/acs.inorgchem.8b03364](https://doi.org/10.1021/acs.inorgchem.8b03364).
- [52] Hou, X.; Wang, F.; Han, L.; Pan, X.; Li, H.; Yang, Y.; Roesky, H. W. Self-Assembly of Discrete Copper(I)–Halide Complexes with Diacylthioureas. *Z Anorg. Allg. Chem.* **2018**, 644, 142–148. DOI: [10.1002/zaac.201700430](https://doi.org/10.1002/zaac.201700430).
- [53] Sahoo, S. K.; Khatun, N.; Jena, H. S.; Patel, B. K. Stable Cu(I) Complexes with Thioamidoguanidine Possessing Halide–Bridge Structure. *Inorg. Chem.* **2012**, 51, 10800–10807. DOI: [10.1021/ic301429g](https://doi.org/10.1021/ic301429g).
- [54] Siemeling, U.; Vorfeld, U.; Neumann, B.; Stammler, H.-G. Cuprophilicity? A Rare Example of a Ligand-Unsupported CuI–CuI Interaction. *Chem. Commun.* **1997**, 18, 1723–1724. DOI: [10.1039/A702793A](https://doi.org/10.1039/A702793A).
- [55] Harisomayajula, N. V. S.; Makovetskiy, S.; Tsai, Y.-C. Cuprophilic Interactions in and Between Molecular Entities. *Chem. Eur. J.* **2019**, 25, 8936–8954. DOI: [10.1002/chem.201900332](https://doi.org/10.1002/chem.201900332).
- [56] Lu, W.; Yan, Z.-M.; Dai, J.; Zhang, Y.; Zhu, Q.-Y.; Jia, D.-X.; Guo, W. J. Coordination Assembly of TTF Derivatives Through CuI Bridges. *Eur. J. Inorg. Chem.* **2005**, 19, 2339–2345. DOI: [10.1002/ejic.200401002](https://doi.org/10.1002/ejic.200401002).
- [57] Noren, B.; Oskarsson, A. Bond Length Variations in Tetrahydrothiophene Solvates of the Coinage Metals: The Crystal Structure of di- μ -Iodo-Bis[Bis(Tetrahydrothiophene) Copper(I)]. *Acta Chem. Scand.* **1987**, 41, 12A–17A.
- [58] Ndiaye, A. L.; Guyon, F.; Knorr, M.; Huch, V.; Veith, M. Modification of the Hydrogen Bonds Network in a Hydroxyl Functionalized Dithiolene Ligand by HgX_2 Complexation. *Z Anorg. Allg. Chem.* **2007**, 633, 1959–1963. DOI: [10.1002/zaac.200700134](https://doi.org/10.1002/zaac.200700134).
- [59] Raper, E. S.; Creighton, J. R.; Bell, N. A.; Clegg, W.; Cucurull-Sánchez, L. Complexes of Heterocyclic Thiones and Group Twelve Metals Part I. Preparation and Characterisation of 1:1 Complexes of Mercury(II) Halides with 1-Methylimidazoline-2(3H)-Thione: The Crystal Structure of $[(\mu_2$ -Dibromo)Bis(Trans{(Bromo)(1-Methyl-Imidazoline-2(3H)-Thione)}Mercury(II))] at 160 K. *Inorg. Chim. Acta* **1998**, 277, 14–20. DOI: [10.1016/S0020-1693\(97\)06052-0](https://doi.org/10.1016/S0020-1693(97)06052-0).
- [60] Popović, Z.; Pavlović, G.; Soldin, Ž.; Popović, J.; Matković-Čalogović, D.; Rajić, M. 1:1 And 1:2 Complexes of Mercury(II) Halides with 1,3-Thiazolidine-2-Thione. Spectral, Thermal, and Crystal Structure Studies. *Struct. Chem.* **2002**, 13, 415–424. DOI: [10.1023/A:1020541602675](https://doi.org/10.1023/A:1020541602675).
- [61] Karri, R.; Chalana, A.; Das, R.; Rai, R. K.; Roy, G. Cytoprotective Effects of Imidazole-Based [S1] and [S2]-Donor Ligands against Mercury Toxicity: A Bioinorganic Approach. *Metallomics* **2019**, 11, 213–225. doi:[10.1039/c8mt00237a](https://doi.org/10.1039/c8mt00237a).
- [62] Rogers, R. D.; Bond, A. H.; Wolff, J. L. Structural Studies of Polyether Coordination to Mercury(II) Halides: Crown Ether versus Polyethylene Glycol Complexation. *J. Coord. Chem.* **1993**, 29, 187–207. DOI: [10.1080/00958979308037425](https://doi.org/10.1080/00958979308037425).
- [63] Mahmoudi, G.; Stilinović, V.; Gargari, M. S.; Bauzá, A.; Zaragoza, G.; Kaminsky, W.; Lynch, V.; Choquesillo-Lazarte, D.; Sivakumar, K.; Khandar, A. A.; Frontera, A. From Monomers to Polymers: Steric and Supramolecular Effects on Dimensionality of Coordination Architectures of Heteroleptic Mercury(II) Halogenide–Tetradentate Schiff Base Complexes. *Cryst. Eng. Commun.* **2015**, 17, 3493–3502. DOI: [10.1039/C5CE00382B](https://doi.org/10.1039/C5CE00382B).
- [64] Beheshti, A.; Sadat Mousavifard, E.; Kubicki, M.; Grzeškiewicz, A.; Elham Rezatofighi, S. Tuning the Structure of Mercury(II) Complexes as Antibacterial Agents by Varying the Halogen Atoms (Cl and Br) and Extending the Spacer Length of the Imidazole-2-Thione Ligands. *Inorg. Chim. Acta* **2021**, 514, 120010. DOI: [10.1016/j.ica.2020.120010](https://doi.org/10.1016/j.ica.2020.120010).
- [65] Dolomanov, O. V.; Bourhis, L. J.; Gildea, R. J.; Howard, J. A. K.; Puschmann, H. OLEX2: A Complete Structure Solution, Refinement and Analysis Program. *J. Appl. Crystallogr.* **2009**, 42, 339–341. DOI: [10.1107/S0021889808042726](https://doi.org/10.1107/S0021889808042726).
- [66] Sheldrick, G. M. SHELXT-Integrated Space-Group and Crystal-Structure Determination. *Acta Crystallogr. A* **2015**, 71, 3–8. DOI: [10.1107/S2053273314026370](https://doi.org/10.1107/S2053273314026370).
- [67] Sheldrick, G. M. Crystal Structure Refinement with SHELXL. *Acta Crystallogr. C* **2015**, 71, 3–8. DOI: [10.1107/S2053229614024218](https://doi.org/10.1107/S2053229614024218).